Mechanotropic bZIP localization is associated with thigmomorphogenic and secondary cell wall associated gene expression

Joshua H. Coomey[1,2], Kirk J.-M. MacKinnon[1,3], Ian W. McCahill[1,2], Bahman Khahani[1,2], Pubudu P. Handakumbura[1,2], Gina M. Trabucco[1,3], Jessica Mazzola[1], Nicole A. Leblanc[1], Rithany Kheam[1], Miriam Hernandez-Romero[1,2], Kerrie Barry[4], Lifeng Liu[4], Ji E. Lee[4], John P. Vogel[4], Ronan C. O'Malley[4], James J. Chambers[5], Samuel P. Hazen[1,2,3]

[1]Biology Department, University of Massachusetts, Amherst, MA 01003, USA,

[2]Plant Biology Graduate Program, University of Massachusetts, Amherst, MA 01003, USA,

[3]Molecular and Cellular Biology Graduate Program, University of Massachusetts, Amherst, MA 01003, USA,

[4]DOE Joint Genome Institute, Berkeley, CA 94720, USA,

[5]Institute for Applied Life Science, University of Massachusetts, Amherst, MA 01003, USA,

Author for correspondence:
Samuel P. Hazen, hazensam@umass.edu

ORCID
Joshua H. Coomey, https://orcid.org/0000-0001-5866-6671
Kirk J.-M. MacKinnon, https://orcid.org/0000-0001-9698-3985
Bahman Khahani, https://orcid.org/0000-0003-4499-2825
Pubudu P. Handakumbura, https://orcid.org/0000-0002-1708-8315
Kerrie Barry, https://orcid.org/0000-0002-8999-6785
Ji E. Lee, https://orcid.org/0000-0001-8325-1689
John P. Vogel, https://orcid.org/0000-0003-1786-2689
James J. Chambers, https://orcid.org/0000-0003-3883-8215
Samuel P. Hazen, https://orcid.org/0000-0001-9131-8994

AUTHOR CONTRIBUTIONS

JC, IM, and SH conceived and designed the study. JC, IM, PH, GT, MH-R, JV, RO developed techniques and reagents. JC, IM, JM, NL, RK, KB, LL, JL, JV. and RO acquired the data. JC, KM, IM, BK, and SH analyzed and interpreted the data. JC, KM, IM, and SH drafted the manuscript. SH agrees to serve as the author responsible for contact and ensures communication.

Abstract

Plant growth is mediated by the integration of internal and external cues, perceived by cells and transduced into a developmental program that gives rise to cell division, elongation, and wall thickening. Extra-, inter-, and intra- physical cellular forces contribute to this regulation. Across the plant kingdom thigmomorphogenesis is widely observed to alter plant morphology by reducing stem height and increasing stem diameter. The root transcriptome is highly responsive to touch, including components of calcium signaling pathways and cell wall modification. Here, we present data on a mechanotropic bZIP transcription factor involved in this process in grasses. *Brachypodium distachyon* SECONDARY WALL INTERACTING bZIP (SWIZ) protein translocated into the nucleus in response to mechanical stimulation. Misregulation of *SWIZ* expression resulted in plants with reduced stem and root elongation, and following mechanical stimulation, increased secondary wall thickness. Classical touch responsive genes were upregulated in *B. distachyon* roots following touch, and we observe significant induction of the glycoside hydrolase 17 family, which may be indicative of a facet of grass thigmomorphogenesis. SWIZ protein binding to an E-box variant in exons and introns was associated with immediate activation followed by repression of gene expression. Thus, SWIZ is a transcriptional regulatory component of thigmomorphogenesis, which includes the thickening of secondary cell walls.

INTRODUCTION

Forces both internal and external to a cell influence growth. Turgor pressure in conjunction with anisotropic cell wall dynamics determine direction of growth and thus cell shape. Force perception between neighboring cells plays a critical role in the development and maintenance of tissue form and function, such as the lobed, interlocking, pavement cells on the leaf epidermis, or the developmental hotspots in the apical meristem (Hamant et al., 2008; Uyttewaal et al., 2012; Bidhendi et al., 2019). Specific inter-cell forces result in dynamic remodeling of the cortical cytoskeleton, with subsequent changes in cellulose microfibril alignment and alterations to other cell wall components such as pectin methyl esterification (Hamant et al., 2008; Uyttewaal et al., 2012; Bidhendi and Geitmann, 2018; Altartouri et al., 2019; Bidhendi et al., 2019). The classic hallmarks of touch responsive growth, or thigmomorphogenesis, include reduced plant height, increased radial growth in plants with a cambial meristem, increased branching, and delayed flowering time (Jaffe, 1973; Biro et al., 1980; Jaffe et al., 1980; Braam, 2004). These attributes have been leveraged by farmers for hundreds of years. As early as 1680 records show Japanese farmers tread on young wheat and barley seedlings to elicit increased branching, spikes per plant, and grain weight per plant, along with stronger roots (Iida, 2014). This practice, known as mugifumi, continues today with mechanized rollers. Thigmomorphogenesis in belowground tissues have also been studied to some extent, with the impact of stiffer substrates eliciting changes in root length and straightness, with the implication of hormonal signaling pathways in mediating this response (Lourenço et al., 2015; Lee et al., 2019; Nam et al., 2020). The known

touch responsive mutants in *A. thaliana* have more skewed roots than wild type when grown on stiff inclined media (Zha et al., 2016).

Calcium is a critical cellular signaling molecule, and cytosolic Ca^{2+} fluctuations are induced by mechanical stimuli and implicated in mechanosignaling (Monshausen et al., 2009; Szczegielniak et al., 2012). Mechanical stimulus can significantly remodel gene expression (Braam and Davis, 1990; Braam, 2004; Lee et al., 2005). The so-called *TOUCH* (*TCH*) genes in *Arabidopsis thaliana*, encode calmodulin (*AtTCH1*/*AtCaM2*), calmodulin-like proteins (*AtTCH2*/*AtCML24*, *AtTCH3*/*CML12*), and a xyloglucan endotransglucosylase/hydrolase (*AtTCH4*/*AtXTH22*) (Braam and Davis, 1990). Touch responsive gene expression patterns often overlap with other stimuli such as dark, cold, and hormone treatment (Polisensky and Braam, 1996; Lee et al., 2005). In addition to calcium binding and signaling, genes related to cell wall modification and a variety of transcription factors and kinases are regulated by mechanical stimulus, as well as genes involved in hormone homeostasis and signaling.

Group I bZIPs are also implicated in mechanosensing. VIRE2-INTERACTING PROTEIN 1 (AtVIP1) and related Group I bZIP proteins translocate from the cytoplasm to the nucleus in response to a variety of biotic and abiotic stimuli, including hypo-osmotic conditions (Tsugama et al., 2012; Tsugama et al., 2014; Tsugama et al., 2016). This translocation appears to be dependent on protein phosphorylation, either from MITOGEN ACTIVATED PROTEIN KINASE 3 during pathogen invasion, or via calcium dependent protein kinases (CDPK). AtVIP1 interacts with calmodulins, the calcium binding proteins involved in many calcium signaling events. The Group I bZIP *Nt REPRESSOR OF SHOOT GROWTH* (*NtRSG*) in tobacco plays a role in maintaining GA homeostasis, wherein it translocates from the cytoplasm to the nucleus in response to cellular bioactive GA levels (Igarashi et al., 2001; Ishida et al., 2008; Fukazawa et al., 2010). Under standard conditions, NtRSG is largely localized in the cytoplasm, and to some extent in the nucleus, where it directly activates expression of *NtEnt-kaurene oxidase*, an enzyme at an early step in the GA biosynthesis pathway. After cellular GAs were chemically inhibited, NtRSG translocated to the nucleus and also activated *NtGA20oxidase1* (*NtGA20ox1*), an enzyme further downstream in the GA biosynthesis pathway that is in part responsible for converting GA species to their bioactive form (Fukazawa et al., 2010; Fukazawa et al., 2011). This suggests that nuclear-localized NtRSG acts to promote bioactive GA synthesis in response to low GA conditions. As with AtVIP1, NtRSG translocation relies on CDPK mediated phosphorylation (Ishida et al., 2008; Ito et al., 2017). Both AtVIP1 and NtRSG associate with 14-3-3 proteins in the cytoplasm while phosphorylated (Ishida et al., 2004; Ito et al., 2014; Ito et al., 2017; Tsugama et al., 2018). Phosphatase activity causes NtRSG and the related AtbZIP29 to dissociate from the 14-3-3 protein and enter the nucleus (Van Leene et al., 2016). *NtRSG* is named for the dwarf phenotype observed when a dominant negative form of the protein is overexpressed. In these dwarf plants, there were reduced levels of bioactive GA and reduced elongation of stem internode cells (Fukazawa et al., 2000).

The development of secondary cell walls is a distinct and critical developmental process in plant growth. Following cellular elongation, some cells, particularly in vascular and structural tissues, increase their mechanical strength by depositing a thick layer of rigid material between the plasma membrane and primary cell wall. These secondary walls are made of crystalline cellulose interwoven with hemicelluloses and phenolic lignin polymers. Although functionally similar, secondary walls in monocotyledonous plants have key differences from those in eudicots, including distinct hemicellulose chemistry and differences in lignin biosynthesis. Grasses also produce mixed-linkage glucans (MLGs), a wall polysaccharide that is rarely found outside the commelinid monocots (Coomey et al., 2020). The synthesis and deposition of secondary wall polymers is tightly controlled spatially and temporally by a well defined transcriptional regulatory network. Evidence in both eudicots and grasses suggest a system of feed-forward loops regulating transcription of wall synthesizing enzymes, with NAC family transcription factors activating wall synthesis genes as well as MYB family and other transcription factors that further promote secondary wall synthesis (McCahill and Hazen, 2019). These networks are very similar between grasses and eudicots, with some components in each that have yet to be described in the other (Coomey et al., 2020). There are currently no bZIP family members in any secondary wall regulatory model.

Beyond differences at the chemical and regulatory levels, grasses employ a fundamentally different growth mechanism than eudicots. Grasses do not have a cambium layer, and thus no lateral meristem. Stem elongation comes from cellular division and elongation in a discrete series of intercalary meristems, called nodes, with one internode region elongating and pushing up subsequent nodes. Detailed studies of thigmomorphogenesis have been conducted almost exclusively in eudicots However, recent work in the model cereal grass *Brachypodium distachyon* shows general overlap with conventional dicot thigmomorphogenesis, albeit with some notable differences, such as no change in stem diameter and increased time to flower (Gladala-Kostarz et al., 2020).

Thigmomorphogenesis is a widely observed phenomenon that results in reduced height, increased radial growth, and increased branching. The mechanisms behind this form of growth are not yet fully understood, but involve aspects of hormone regulation, Ca^{2+} signaling, Group I bZIP intracellular translocation, and changes in gene expression. Here we describe the transcriptional response to mechanical stimulation and the function of a *B. distachyon* bZIP transcription factor, SECONDARY WALL ASSOCIATED bZIP (Bradi1g17700) and its role in touch response and cell wall biosynthesis.

RESULTS

SWIZ is a Group I bZIP transcription factor and candidate cell wall regulator

To identify genes involved in the regulation of secondary cell wall thickening, transcript abundance was measured in *B. distachyon* leaf, root, and stem tissue (Trabucco et al., 2013). A gene annotated as a bZIP transcription factor, Bradi1g17700, was highly expressed in root and

stem relative to leaf (**Fig 1A**). Bradi1g17700 is also a member of a 112 gene coexpression network (**Supplemental Table S1**) that includes genes highly expressed in the peduncle (Sibout et al., 2017). Phylogenetic analysis of Bradi1g17700, hereinafter referred to as *SECONDARY WALL INTERACTING bZIP* (*SWIZ*), amino acid sequence shows it to be an ortholog of the *A. thaliana* Group I bZIPs (Jakoby et al., 2002; Dröge-Laser et al., 2018), and closely related to *AtbZIP18* and *AtbZIP52* (**Fig 1B, File S1**).

SWIZ translocates into the nucleus in response to mechanical stimulus

Group I bZIPs in *A. thaliana* have been described as playing intersectional roles in regulating growth and development, and in doing so display dynamic translocation between the cytosol and the nucleus in response to external cellular force. As an ortholog of these mechanotropic proteins, we hypothesized that SWIZ protein may similarly translocate within the cell in response to mechanical force and contribute to plant growth regulation. To test this, the roots of transgenic plants overexpressing either *SWIZ* fused to *GFP* (*SWIZ:GFP-OE*) or *GFP* alone (*GFP-OE*) were observed following a mechanical stimulus (**Fig 2A**). In control plants, GFP signal was present in both the cytosol and nucleus, which remained constant over the imaging period (**Fig 2B**). GFP signal was mostly observed in the cytosol in *SWIZ:GFP-OE* plants, but following mechanical stimulus, nuclear GFP signal increased substantially, reaching a peak around 30 min post stimulus and returned to near basal levels by about 60 min, while untouched plants showed no change in signal localization (**Fig 2B**).

The dynamics and repeatability of SWIZ nuclear translocation were further investigated by sequential stimulus treatments. Touch response to stimulus can saturate at a certain number of treatments (Martin et al., 2010; Leblanc-Fournier et al., 2014; Moulia et al., 2015). To test if SWIZ translocation dynamics varied after repeated treatments, we applied mechanical force to *SWIZ:GFP-OE* roots at regular intervals. A second stimulus was given 90 min after the first, and a third at 180 min. Following each mechanical stimulation, SWIZ consistently translocated from cytoplasm to nucleus (**Fig 2D**). This suggests that SWIZ translocation dynamics are not impacted by repeated stimulus events 90 min apart.

When conducting these translocation assays, root tissue in the field of view was treated with mechanical force and nuclei in that region were tracked and quantified for fluorescence. To determine if the signal triggering SWIZ translocation is spread beyond the specifically stimulated region, two regions of the same *SWIZ:GFP-OE* root separated by 3 cm were simultaneously observed. The stimulated region showed typical SWIZ:GFP nuclear signal accumulation and in the region below no translocation was observed (**Fig 2C**). At 120 min, the treatments were reversed, with the lower root region receiving a stimulus while the upper region was unperturbed. The lower region showed SWIZ:GFP nuclear translocation while the upper region did not. Thus, the touch stimulus perceived by SWIZ is localized directly to the perturbed region.

Transcriptional response to touch

Having established the nuclear translocation of SWIZ in response to touch, we then investigated what effect touch and SWIZ overabundance during touch may have on gene expression. To assess this, we measured transcript abundance by sequencing mRNA from wildtype and *SWIZ-OE* root tissue just prior to touch (0 min) and at 10, 30, and 60 min following touch treatment (**Fig 3A**). Principal component analysis of transcript abundance shows the greatest amount of variance is attributed to the first principal component, 60%, where samples cluster based on genotype (**Fig 3B**). The second principal component, which accounts for 17% of the variance, distinguished between pre-touch and 10 min following touch, with the last two time points clustering similarly.

The wildtype transcriptome was massively remodeled in response to touch, with 8,902 transcripts differentially expressed ($q < 0.1$) at 10 min post touch, 5,682 transcripts at 30 min, and 7,672 transcripts at 60 min (**Supplemental Tables 2-4**). Touch response studies in *A. thaliana* describe similar changes that include numerous calmodulin (CAM), calmodulin-like (CmL), and xyloglucan endo-transglycosylase/hydrolase (XTH) activity (**Fig 3C**)(Braam and Davis, 1990; Lee et al., 2005). Based on homology with *TCH1*, *TCH2*, and *TCH3*, 79 CAM and CmL genes were identified, the majority of which showed upregulation in wildtype plants following touch treatment (**Supplemental Table 5**). Similarly, homology with *TCH4* identified 37 *B. distachyon XTH* and *XTH-like* genes. Of these, 8 genes were upregulated by touch in wildtype plants, including the two with the highest similarity to *TCH4* (Bradi1g33810 and Bradi33840) (**Fig 3C**, **Supplemental Table 6**). Since xyloglucans are in relatively low abundance in grass cell walls compared to eudicots, we also investigated the effect of touch on other families of the glycosyl hydrolase superfamily (Tyler et al., 2010). In particular, GH17 genes were differentially regulated following touch. The GH17 family is broadly described as modifying β-1,3-glucans. We observed measurable transcript abundance for 35 of the 53 annotated GH17 family members, with 8, 11, and 16 members showing differential expression at 10, 30 and 60 min respectively. Fisher's exact test determined significant enrichment of GH17 expression at time 60 ($p = 9.307e\text{-}3$) (**Fig 3C**, **Supplemental Table 7**). Online resources are available to explore the RNA-seq data at (https://hazenlab.shinyapps.io/swiztc/), which provides an interactive platform for interrogating the *B. distachyon* touched-root transcriptome.

Cell wall genes are downregulated immediately following touch, then induced concurrent with SWIZ nuclear translocation and more strongly in *SWIZ-OE*

Genes related to secondary cell wall synthesis were immediately downregulated in wildtype plants following touch, but were subsequently upregulated (**Fig 4**). Xylan, cellulose, MLG, and callose synthesis associated genes were upregulated 30 and 60 min following touch, while lignin biosynthesis and BAHD acyltransferase genes were upregulated at 60 min. Network analysis of gene expression patterns over time using the iDREM software showed that in *SWIZ-OE* plants, cell wall genes were more rapidly induced (**Supplemental Fig 2A-B**). Prior to touch, nearly all of the cell wall associated genes investigated were significantly downregulated relative to

wildtype, then significantly upregulated following touch (**Fig 4**). In *SWIZ-OE*, cell wall related terms were enriched in paths that had stronger upregulation earlier than the same terms in wildtype (**Supplemental Fig 2A-B**). Notably, aspects of cell wall polysaccharide biosynthesis, particularly glucan biosynthesis, were significantly enriched in *SWIZ-OE* path D, while not significantly enriched in wildtype (**Supplemental Table 8**). This is mirrored when looking at specific gene expression, with primary wall associated CESAs, MLG, and callose synthesis genes all significantly upregulated following touch in *SWIZ-OE*. Thus, cell wall genes were immediately repressed by touch, followed by significant activation. That activation occurs more rapidly in *SWIZ-OE* plants and is associated with the timing of SWIZ protein nuclear translocation.

SWIZ protein binding in the gene body is associated with dynamic changes in gene expression

Next we investigated the direct binding targets of SWIZ protein by performing DNA affinity purification sequencing (DAP-seq) with whole genomic DNA. In total, SWIZ interacted with 2,455 distinct positions in the genome (**Supplemental Table S9**). Those regions were significantly enriched for two sequence motifs, (A/C)CAGNCTG(T/G) and (A/C)CAGCTG(T/G) that are variants of the E-box motif (**Fig 5A**). A plurality of the binding sites were between the translational start and stop sites with 21% of the peaks in introns and 21% in exons (**Fig 5B**). Fewer than 10% of the peaks occurred in UTRs and the promoter (defined as 5 kb upstream of the 5 'UTR) and intergenic regions each accounted for 25% of the binding sites. Thus, SWIZ protein is preferentially bound to an E-box like motif and often in the gene body (**Fig 5C**).

To investigate the effects of possible SWIZ binding on gene expression, we compared the genes differentially expressed in the *SWIZ-OE* touch response RNA-seq time courses with the promoter and gene body binding targets identified by the DAP-seq assay. Prior to touch, genes with promoter-SWIZ protein interactions were most often downregulated in *SWIZ-OE* relative to wildtype (**Table 1**). However, some SWIZ targets behaved differently following touch. SWIZ promoter binding targets were most often upregulated in *SWIZ-OE* in all three post-touch time points. Thus, SWIZ promoter binding was coincident with repression, but following a touch stimulus, activation was more prominent. However, this difference between untreated and touched was not as pronounced in gene body targets, with more upregulated genes 10 min following touch and more downregulated 30 and 60 min following touch. To further explore these trends we conducted iDREM cluster analysis of the differentially expressed genes that were also SWIZ protein targets (**Fig 5D**). For both wildtype and *SWIZ-OE*, the network analysis revealed a pathway to increased gene expression by 60 min following touch. The network pathway trend for both promoter and gene binding targets in wildtype was immediate repression at 10 min followed by increased expression at 30 and 60 min post-stimulus. A unique pathway was observed among gene body binding targets in *SWIZ-OE*; transcript abundance was reduced

following touch. Thus, SWIZ binding to a promoter or gene body was more strongly associated with increased expression with the exception of gene body targets in touched *SWIZ-OE* plants, which were more strongly repressed.

Among the genes differentially expressed in response to both touch, *SWIZ-OE* transgene, and bound by SWIZ in the first intron is the mixed glucan synthase *CSLF6* (**Fig 6A**). The transcript abundance of *GA2ox3*, which inactivates bioactive GA, was bound by SWIZ protein in both the gene body and 3'UTR and expression significantly increased 30 min after touch in *SWIZ-OE* (**Fig 6B**). An example of gene body binding repression is SWAM3 (Bradi1g30252), the closest ortholog to a wheat transcription factor induced by hypoxia, *TaMYB1* (Lee et al., 2006; Handakumbura et al., 2018). This gene was touch induced in wildtype and repressed in *SWIZ-OE* with a binding site in the 5'UTR (**Fig 6C**). A membrane-associated transcription factor, NAC35, exhibited a similar expression to *SWAM3* (Handakumbura et al., 2018) and SWIZ bound the promoter region (**Fig 6D**).

Cis-regulatory sequences associated with mechanical stress, wounding, and cell wall synthesis are enriched among touch responsive genes

Genes differentially expressed in wild-type in response to touch were analyzed for enrichment of putative *cis*-regulatory elements (CREs). We identified several sequences significantly enriched among touch-responsive transcripts (**Fig 7, Supplemental Fig 6, Supplemental Table S10 and S11**). Several of those have been previously described as touch responsive, including the Rapid Stress Response Element, the GCC boxes AGCCGCC and GCCGCC, a sequence referred to as both the E-box and G-box (CACGTG), CM2, AP2-like, GGNCCCAC site II element, P-box, and the GRF and FAR1 binding sites (Rushton et al., 2002; Walley et al., 2007; Doherty et al., 2009; Fernández-Calvo et al., 2011; Moore et al., 2022). Other putative CREs have not previously been identified as touch responsive. One CRE was exclusively enriched in touch repressed genes at all time points, the TCP site II element TGGGC. A GATA-like binding site was enriched among 10 min repressed transcripts. The homeobox binding site (motif) was enriched among both induced and repressed genes. The CGCG-box was enriched among induced genes at all timepoints similar to RSRE, CM2, and FAR1. The two CREs known to play a prominent role in protein-DNA interactions that regulate secondary cell wall thickening were also significantly enriched (Coomey et al., 2020). The VNS element was enriched among induced genes, and the AC element ACC(A/T)ACC had a unique profile where it was enriched among repressed genes at 10 min, enriched in both induced and repressed genes at 30 min, and among induced genes only at 60 min.

Root morphology is altered by *SWIZ-OE* and touch treatment

Given the SWIZ protein mechanotropic response and regulatory influence, we then investigated how SWIZ might impact plant growth in response to touch. We challenged wildtype and *SWIZ-OE* roots with the same style of touch treatment used in the translocation and gene expression experiments, but repeated twice daily for a period of five days. In both touch and control conditions, *SWIZ-OE* roots were significantly shorter than wildtype, suggesting a dwarfing effect

from *SWIZ* overabundance (**Fig 8A-C**). Mechanical challenges to roots have been reported to impact root straightness, a trait that has also been described as being impacted in other bZIP studies (Van Leene et al., 2016; Zha et al., 2016). In control conditions, we observed that *SWIZ-OE* roots were significantly less straight than wildtype, while this was not observed in in response to touch (**Fig 8D**). We further tested the mechano-response of *SWIZ-OE* roots by growing seedlings on plates with increasing degrees of plate angle at 10°, 20°, 30°, and 40° from vertical (**Fig 9**). Greater angles result in more direct contact between the root tip and media and thus increased mechanical stimulation in *A. thaliana* (Oliva and Dunand, 2007; Zha et al., 2016). Wildtype *B. distachyon* roots displayed decreasing root length with increasing plate angle. *SWIZ-OE* roots were shorter than wildtype at all plate angles tested (**Fig 9**). Root straightness did not show any significant differences. Thus, *SWIZ-OE* roots were shorter than wildtype regardless of direct touch stimulus or increasing plate angle, and significantly less straight under direct touch.

B. distachyon displays classic thigmomorphogenic phenotypes

We next investigated the effect of touch treatment on aboveground tissue. Wildtype plants were perturbed with a metal bar once every 90 min for either two or three weeks (**Supplemental Fig 3, 4**). After the treatment period, all plants were allowed to recover and grow undisturbed until senescence (**Supplemental Fig 4**). Two week stressed plants were significantly shorter than control plants, and three week stressed plants were shorter still (**Supplemental Fig 4A-B**). Despite this difference in height, there was not a significant difference between the groups in terms of aboveground plant weight (**Supplemental Fig 4C)**. Three week stressed plants had significantly more branches ($p < 0.05$), with a non-significant increase in two week stressed plants (**Supplemental Fig 4D**). Transverse stem cross sections in the third elongated internode and peduncle did not show a significant difference in cell wall thickness or phloroglucinol staining in response to touch (**Supplemental Fig 4E-G**).

Stem height and cell wall thickening are affected by *SWIZ-OE* and touch treatment

To test the role of *SWIZ* in regulating thigmomorphogenesis and secondary cell wall development, we tested wildtype and *SWIZ-OE* under two weeks of mechanical perturbation as described above. In control conditions, there were no differences among genotypes in height, weight, or branching. Touch significantly shortened both wildtype and *SWIZ-OE* stems relative to control conditions, but not relative to each other (**Fig 10A, Supplemental Fig 5**). Thus, *SWIZ-OE* stems are inherently shorter than wildtype. Transverse sections of the stem were made in the peduncle, the last elongated stem internode where the touch treatment occurred during stem elongation, and stained with phloroglucinol-HCl. *SWIZ-OE* touched peduncles showed significantly thicker interfascicular fiber cell walls compared to untouched(**Fig 10B-C**). Thus, overabundance of *SWIZ* transcript sensitized wall thickening in response to touch treatment.

DISCUSSION

Touch stimulus is generally an inhibitor of plant elongation growth, but promotes branching and radial expansion (Jaffe, 1973; Braam, 2004; Chehab et al., 2009). The majority of this work has been done in dicots, where increased radial growth has been associated with greater deposition of secondary wall forming cells, particularly in woody species such as poplar (Biro et al., 1980; Coutand et al., 2009; Börnke and Rocksch, 2018; Roignant et al., 2018; Niez et al., 2019). Our understanding of thigmomorphogenesis in grasses is limited, and mostly in the agricultural context of lodging (Shah et al., 2019). While these studies highlight the importance of stem strength and associated cell wall defects, they do relatively little to elucidate the mechanosensitive response. Recent work by Gladala-Kostarz et al (2020) describes grass touch response to both wind and direct mechanical treatment, with an emphasis on cell walls and stem anatomy. Touch treatment significantly increased lignin content, and also altered the relative abundance of wall bound hydroxycinnamates. Wall polysaccharide content, particularly glucose and galactose, also increased. Consistent with increased secondary wall lignification, touched plants had increased wall stiffness and decreased saccharification.

Specific gene expression patterns have become molecular hallmarks of plant touch response, most notably induction of the *TCH* and similar genes. Orthologs of wall modifying XTHs and CAM/CML signaling genes are upregulated in response to mechanical stimulation across species, and as we present here, in *B. distachyon*. Touch elicits major global changes in gene expression, with 2.5% to 10% of the genes assayed in *A. thaliana* and poplar differentially expressed (Lee et al., 2005; Pomiès et al., 2017; Van Moerkercke et al., 2019). In sorghum (*Sorghum bicolor*), leaf sheath imposes mechanical constraints on emerging buds, and removing this dramatically altered gene expression, with 42% of genes differentially expressed over a 9 h period (Liu and Finlayson, 2019). Our observations of short term (<2 h) touch responses within stress related pathways align with observations from poplar and *A. thaliana*, with rapid induction of *TCH*, biotic, and abiotic stress related genes (Pomiès et al., 2017). Canonical touch responsive genes such as the orthologs of *TCH1-4* and related *XTH* and *CML* genes were upregulated immediately following stimulus. However, we also note the previously unreported touch-induction of GH17 family genes, as well as *CSLF6*, suggesting a role for MLG and β-1,3 glucan modification in grass touch response.

In both poplar and in our analysis of *B. distachyon* touch responses, touch-regulated expression of secondary cell wall related transcripts differed between early and late timepoints. Upon touch, we observed immediate repression of many key cell wall biosynthetic enzymes, followed by significant upregulation one hour after stimulus. In poplar, no significant repression of these transcripts was reported, but terms related to wood or cell wall synthesis were also not enriched among touch-regulated transcripts until 24 or 72 hours after touch (Pomiès et al., 2017). While differences in the method used to quantify gene expression, and in the temporal sampling scheme complicate direct comparisons of plant touch response experiments, this may suggest that

delayed induction of secondary cell wall transcripts is a common feature of plant touch responses.

Thigmomorphogenesis and secondary cell walls

Our understanding of touch responsive gene expression is further informed by the dynamics of SWIZ nuclear translocation. The timing of SWIZ nuclear accumulation following mechanical stimulus was consistent with observations of *A. thaliana* Group I bZIPs (Tsugama et al., 2014; Tsugama et al., 2016). However, by adopting a finer temporal sampling scheme, and quantifying nuclear signal sooner after touch (2 vs. 30 min), our results clarify the rapid and immediate nature of this translocation. Furthermore, we show that the speed and magnitude of SWIZ nuclear accumulation is not diminished over three successive touch treatments. Notably, poplar transcriptional responses to a second touch stimulus were significantly attenuated relative to a single treatment, and in separate experiments, trees subjected to a daily touch treatment over four days no longer showed touch-induced increases in their rates of radial growth (Martin et al., 2010; Pomiès et al., 2017). Thus, if *B. distachyon* is likewise desensitized to repeated touch, the high repeatability of SWIZ translocation might implicate a mechanism downstream of touch perception and bZIP translocation in mediating that shift. Like the touch-responsive transcription factor AtVIP1, SWIZ translocation occurred in the specific area of touch treatment, suggesting a local response to stimulus rather than a tissue or whole organism response. *SWIZ-OE* roots were shorter than wildtype under control, direct touch, and multiple plate growth angles. This may suggest that *SWIZ-OE* roots grown in agar media experience a sufficient degree of mechanical input to reduce elongation.

Another component of this reduced elongation may be increased secondary cell wall deposition, as this could terminate elongation. The CREs enriched among genes induced or repressed by touch revealed an overlap between CREs previously associated with wounding such as the RSRE and CM2 and more subtle touch treatments. Two CREs not previously associated with touch response, the AC and VNS elements, are DNA targets of MYB and NAC transcription factors that regulate the thickening of secondary cell walls (Ohtani et al., 2011; Zhong et al., 2011; Kim et al., 2012; Zhong and Ye, 2012; Handakumbura et al., 2018; Olins et al., 2018). These CREs may be the target of wall biosynthesis genes that were touch responsive and differentially expressed in *SWIZ-OE*.

Prior to touch, almost the entire monolignol biosynthetic pathway, including laccase genes that radicalize monolignols, and BAHD acyltransferases that add hydroxycinnamic acids to wall polymers, are significantly downregulated in *SWIZ-OE* plants. Following touch, most of these genes become significantly upregulated. This activity is consistent with our observations of increase in wall thickness in touched *SWIZ-OE* peduncles, and aligns with the compositional data presented by Gladala-Kostarz et al. (2020). This activation may be a result of direct binding of SWIZ to modulate expression, or an indirect effect from another transcriptional regulator such as

the NAC transcription factor *SWN5* that is significantly upregulated in *SWIZ-OE* following touch and capable of activating the full developmental program for secondary cell wall synthesis (Valdivia et al., 2013). While the E-box (CANNTG) was initially described as a bHLH binding motif, many bZIP groups in *A. thaliana* have been shown to bind similar sequences. The two closets *A. thaliana* orthologs of SWIZ , bZIP18 and 52, both bind (A/C)CAG(G/C)(T/C), while VIP1 binds (A/C)CAGCT(G/A) (O'Malley et al., 2016). Using the same technique, we identified the SWIZ binding motifs as (A/C)CAGNCTG(T/G) and (A/C)CAGCTG(T/G). Both of these sequences are similar to those bound by *A. thaliana* orthologs, although the presence of an ambiguous nucleotide in the core of one variant is not previously reported for other Group I bZIPs. Among genes bound by SWIZ *in vitro,* we observed both activation and repression following touch, suggesting a complex regulatory function for SWIZ. Furthermore, SWIZ direct binding sites were found in both promoter regions and in the body of genes and most often in genes activated by touch. SWIZ gene body binding targets tended to be repressed in *SWIZ-OE* plants following touch, without either being clearly associated with up or down regulation. AtVIP1 and AtbZIP29 have both been described as activators, particularly of genes related to biotic and abiotic stress response, cell cycle control, and development. (Yin et al., 1997; Ringli and Keller, 1998; Pitzschke et al., 2009; Van Leene et al., 2016). AtbZIP18 is described as a repressor of transcription (Tsugama et al., 2012; Gibalová et al., 2017).

bZIPs are known to homo- and heterodimerize through their leucine zipper domains (Schütze et al., 2008), and in *A. thaliana* the combinatorial interactions of different bZIP groups have been fairly well described (Deppmann et al., 2004; Ehlert et al., 2006; Grigoryan and Keating, 2006; Weltmeier et al., 2006; Schütze et al., 2008). These interactions can have a synergistic effect on transcriptional activity, and can result in unique binding interactions (Schütze et al., 2008; Van Leene et al., 2016). It is conceivable that this heterodimerization may explain some aspects of our results, such as why so many of the cell wall genes that are upregulated in *SWIZ-OE* after touch are significantly downregulated prior to touch. One hypothesis is that SWIZ, as with many other bZIPs, can regulate targets as a heterodimer. The abundance of SWIZ protein in the cytoplasm in *SWIZ-OE* plants prior to touch may act as a sink, sequestering interacting partners that would otherwise be regulating targets independent of a touch stimulus. Further experimentation is needed to elucidate this bZIP regulatory network in response to touch and other stimuli.

CONCLUSIONS

Proteins orthologous to SWIZ in other species have been implicated in cell wall development and remodeling, but not cell wall thickening. Touch significantly remodeled the *B. distachyon* transcriptome, with notable changes in wall polysaccharide biosynthetic gene expression not previously reported and revealed an enrichment of secondary cell wall associated CREs, the AC and VNS elements. Enhanced *SWIZ* function through overexpression amplified this touch-responsive gene expression. Together, the evidence presented here connects mechanotropic bZIP dynamics with thigmomorphogenesis and secondary cell wall transcriptional regulation.

MATERIALS AND METHODS

Phylogenetic analysis

Protein sequences described for *A. thaliana*, *B. distachyon*, and *O. sativa* (Liu and Chu, 2015) as Group II bZIPs were selected and searched against the most recent genome annotations in Phytozome v12.1 (https://phytozome.jgi.doe.gov). The *Nicotiana tabacum* homologs NtRSGa and NtRSGb were also added to the analysis. Protein sequences were aligned using the MAFFT service for multiple sequence alignment with the iterative refinement method L-INS-I (Katoh et al., 2019). The alignment was used to construct the phylogenetic tree using a maximum likelihood analysis with a bootstrap resampling value of 1000 in W-IQ-TREE (Trifinopoulos et al., 2016). All of the proteins included in the phylogenetic analysis are described in **Supplemental File 1**.

Plant transformation

Overexpression and artificial microRNA transgenes and transgenic plants were constructed as previously described (Handakumbura et al., 2013). The full length coding sequence of Bradi1g17700 was amplified from cDNA and cloned into the pOL001 ubigate ori1 binary expression vector (Handakumbura et al., 2018) to make the *SWIZ-OE* trangene. The coding sequence lacking the stop codon was amplified and fused in frame with the coding sequence of *Aequorea victoria* enhanced GFP in the pOL001 vector to generate *SWIZ:GFP-OE*.

Translocation assay

Seeds were surface sterilized and grown vertically on 1X MS media, pH 5.7, without sucrose for 6d at 28°C in the dark. After 6 d, seedlings were moved to treatment plates containing 1X MS media, pH 5.7, plus varying concentrations (0, 10, 50, or 100 mM) of GA4, paclobutrazol. Roots were positioned such that they were completely submerged in media and relatively flat along the imaging plane After a 6 h incubation, plants were stimulated and imaged.

All observations were made on a Nikon A1R scanning confocal microscope using a Plan Apo 10x 0.5NA objective. Root areas to be observed were located by eye using transmitted light and then confirmed under confocal conditions using a 488 nm laser and green filtered PMT detector. The X, Y, and Z coordinate stage locations of each region were programmed into the Nikon NIS Elements 5.2 Advanced Research V6 software package for automated imaging. After all target regions were programmed, 30 min of imaging began pre-treatment, with images captured every 2 min.

To elicit the touch response, the observed root region was gently probed 5 times in ~5 sec with a blunt probe while observing through the eyepiece (**Supplemental Fig 7**). Images were captured for 60-90 min post treatment. For experiments with multiple stimulus events, the timelapse sequence was paused and roots were probed as described for the relevant stimulus events.

Analysis of GFP signal was done using the Nikon NIS Elements Advanced Research V5 software package. For each time series, the frame showing maximal nuclear signal was selected and used as a reference point. Using the General Analysis tool, a channel for GFP signal was established and thresholded for intensity and particle size to identify the nuclear regions. These regions were added to the timelapse image series as a binary layer and then converted to static regions of interest for quantification. The GFP intensity under each nuclear region of interest was calculated for the course of the timelapse and the average signal from each nucleus was plotted for intensity over time.

Thigmomatic construction and operation

The Thigmomatic is a basic robotic device that sweeps plants with a metal bar at regular intervals to elicit a touch response. The device was constructed from aluminum V-Slot linear rail (Openbuilders Partstore, Monreoville, NJ) and bracket joints for the upright supports (20x20 mm), cross bars (20x20 mm), and tracks (20x40 mm). Two gantry carts ride along the 20x40 mm V-Slot linear rails, connected by a 6.35 mm diameter metal rod bolted to the carts. Their movement is powered by a belt driven linear actuator system using a NEMA 17 stepper motor with a 12V 18W AC/DC power supply. The stepper motor provides fine spatial control over the gantry cart position with bi-directional motion. Motor function is controlled by a Raspberry Pi 3B microcomputer equipped with a stepper motor HAT (Adafruit Industries, New York). The Thigmomatic was programmed to cover a specified distance in one direction once every 90 min. Accession Bd21-3 was used for these experiments. Seeds were stratified on wet paper towel wrapped in foil to exclude light for 10 days at 4°C before being planted in Promix BX potting mix in SC10 Ray Leach Cone-tainers (Stuewe & Sons Inc). Plants were grown in a Percival PGC-15 growth chamber with day/night conditions of 20 h light at 24°C and 4 h dark at 18°C, respectively.

Transverse stem sections and histology

The main stem of senesced plants was taken and the internode of interest removed and embedded in 8% agarose. A Leica VT1000 Vibratome was used to make 55 µm thick transverse sections. Histochemical staining was carried out using phloroglucinol-HCl as previously described (Matos et al., 2013). Images were obtained at 4, 10, and 20X using a Nikon Eclipse E200MV R light microscope and PixeLINK 3 MP camera. Transverse sections imaged at 20x were used for cell wall thickness measurements. Interfascicular fiber cells separated by one cell layer from the mestome cells on the phloem side of major vascular bundles were targeted for measurement. Using ImageJ, lines were drawn across two walls of adjoining cells. The resulting line length was divided by two to give one cell wall width. Approximately 15 measurements were made for each plant.

RNA extraction and quantification and analysis

Seedlings were grown for 6 d on vertical 1X MS agar plates. Touch treatment was performed as described above using a metal probe along the entire length of the root. Untouched samples were

collected immediately before touch treatment began, and touched samples were collected after the designated time. Three roots were pooled per biological replicate, and RNA was extracted using the Qiagen RNeasy Plant Mini Kit with on-column DNA digestion with RNase-free DNase I (Qiagen). Strand-specific libraries were prepared using the Illumina TruSeq kit. Libraries were sequenced using Illumina technology. Sequences were processed as previously described (MacKinnon et al., 2020). Briefly, the transcripts were checked for quality using FastQC (Andrews, 2010), then aligned to the Bd21 reference genome (v3.1) using HiSat2 (Kim et al., 2015), then assembled and quantified using StringTie (Pertea et al., 2015). Transcripts were normalized and assessed for differential expression using the likelihood ratio test from the R (v3.6.0) package DESeq2 (Love et al., 2014). Benjamini-Hochberg *p*-value adjustments were applied to account for multiple testing with a significance cutoff of 0.1. Of the 34,310 genes in the reference genome, 30,380 had non-zero read counts after normalization. In total there was an average mapping percentage of 97.8% for all libraries, as determined by SAMtools (Li et al., 2009). Specific treatment contrasts (i.e., wildtype vs *SWIZ-OE*) were identified and compared using the Wald test from DESeq2 (Love et al., 2014). Statistical enrichment of gene families was assessed using Fisher's exact test. Raw read data was deposited in the European Nucleotide Archive for public access (Accession no.: E-MTAB-10084).

DNA affinity purification sequencing

DNA affinity purification was carried out as previously described (Handakumbura et al., 2018). In brief, transcription factor coding sequences were HALO tagged and mixed with Bd21 genomic DNA for *in vitro* binding. Protein-DNA was crosslinked, fragmented, immunoprecipitated using the HALO antibody, barcoded, and sequenced. Reads were mapped back to the Bd21 genome using HiSat2 (Kim et al., 2015) to identify binding target loci. Peak calling and motif analysis was done using HOMER v4.10 (Hypergeometric Optimization of Motif EnRichment) suite (Heinz et al., 2010). Motif enrichment was calculated against the hypergeometric distribution; the significance threshold was set to $p < 0.05$. The nearest annotated gene to a bound peak was used for GO analysis. Raw read data were deposited in the European Nucleotide Archive for public access (Accession no.: E-MTAB-10066).

Gene Ontology analysis

Phytozome was used to find orthologs for all *B. distachyon* v3.1 genes as the reciprocal best match to *A. thaliana* TAIRv10 protein sequences. Arabidopsis gene identifiers were submitted to g:Profiler (Raudvere et al., 2019) for KEGG and Wiki pathway enrichment analysis.

iDREM network analysis

Probabilistic graphical models that predict diverging gene expression paths and the points at which regulators may influence those paths were generated using iDREM (Ding et al., 2018). Briefly, this software applies an input-output hidden Markov model to time course gene expression data overlaid with static regulatory information, in this case SWIZ protein-DNA

interactions identified from DAP-seq. GO analysis, described above, was also applied to the gene sets in each path identified by iDREM.

Cis-regulatory sequence analysis

Cis-regulatory sequence analysis of differentially expressed genes after touch was implemented by categorizing them based on an increase or decrease in transcript abundance at each time point. Homer v.4.10 was used to identify regulatory sequences in the 1000 bp upstream of the transcriptional start site of differentially expressed genes previously identified in *A. thaliana* DAP-seq analysis (Heinz et al., 2010; O'Malley et al., 2016). These motifs were visualized using the SeqLogo package. Another approach with different assumptions was implemented as previously described (Moore et al., 2022). In brief, touch-responsive genes were divided into six groups: up or down regulated each at 10, 30, and 60 min after touch. To find putative CREs, 1000 bp upstream of differential expressed genes were retrieved and searched for all possible 6-mers. The growing k-mers approach was conducted to include longer k-mers. For instance, for 7-mers, eight possible situations could be considered for each significant 6-mer, by adding A, T, C and G to each end of a 6-mer. If the *p*-value was lower, the 7-mer(s) was kept; if not, 7-mers were discarded. This growing *k*-mer approach continued until a 12-mer length was reached. The Tomtom tool in MEME Suite 5.4.1 was used to find similarities between significant CREs for each cluster with the *A. thaliana* DAP-seq database. Putative CREs with a false discovery rate less than 0.01 were considered as the best match for known CREs.

Root Touch Experiment

Seeds were surface sterilized and plated on 1x MS, pH 5.7, containing 0.05 % MES as a buffering agent and 1% plant agar (Gold Bio). Seeds were stratified on plates in the dark at 4 ℃ for 2 days and then transferred to a Percival PGC-15 growth chamber with day/night conditions of 16h light at 24 ℃ and 8h dark at 18 ℃, respectively and grown at a ~10° angle from vertical. After 2 days of preliminary growth, a touch location was designated by selecting the lower of 1 cm up from the root tip or 1 cm down from the seed and marked on the plate. Each day for 5 days, this marked spot was treated twice a day, two hours before and two hours after chamber midday (ZT6 and ZT10). Touch treatment consisted of 5 firm presses with the side of a sterile pipette tip, just hard enough to cause elastic deformation of the media underlying the root when viewed through a dissecting microscope. To ensure unbiased application of touch treatment and control for any blocking effects, each plate contained one group of four *SWIZ-OE* seeds and one group of four Bd21-3 wildtype seeds, with the experimenter blinded to their respective positions for the duration of the experiment.

Root length and straightness measurement

Plates were photographed at the conclusion of the experiment. To generate high contrast images suitable for root tracing, plate images were separated into hue, saturation and brightness channels, and the saturation channel was selected and inverted. Semi-automated measurements

of root length were performed using the Smart Roots plugin for ImageJ (Lobet et al., 2011). Straightness was quantified as described in (Swanson et al., 2015); the straight line distance between root tip and the base of the seed was measured, and this value was divided by the traced length of the root.

SUPPLEMENTAL MATERIALS

Supplemental Table S1. Cluster 56 from network analysis of gene expression atlas (Sibout et al. 2017) includes Bradi1g17700.

Supplemental Table S2. Differentially expressed genes in wildtype Bd21-3 root tissue 10 min after touch treatment.

Supplemental Table S3. Differentially expressed genes in wildtype Bd21-3 root tissue 30 min after touch treatment.

Supplemental Table S4. Differentially expressed genes in wildtype Bd21-3 root tissue 60 min after touch treatment.

Supplemental Table S5. Calmodulin and calmodulin-like touch responsive gene expression in wildtype Bd21-3 root tissue.

Supplemental Table S6. XTH and XTH-like touch responsive gene expression in wildtype Bd21-3 root tissue.

Supplemental Table S7. Glycoside hydrolase touch responsive gene expression in wildtype Bd21-3 root tissue.

Supplemental Table S8. GO analysis of genes in iDREM identified pathways derived from differential gene expression following touch in wildtype, swiz-amiRNA, and SWIZ-OE root tissue.

Supplemental Table S9. DAP-seq results of SWIZ genome binding locations.

Supplemental Table S10. All putative CREs enriched in differentially expressed genes at each timepoint identified using the k-mer approach.

Supplemental Table S11. CREs described for Arabidopsis thaliana in O'Malley et al. 2016 that match CREs identified using the k-mer approach.

Supplemental Figure 1. Description of *SWIZ* transgenic reagents. (A) Diagram of *SWIZ* overexpression transgenes. The *ZmUbi* promoter was used to drive expression of the *SWIZ* coding sequence, either alone or fused in frame with *eGFP*. (B) Relative level of *SWIZ* transcript measured by RT-qPCR in whole stem tissue was collected 1 d after inflorescence emergence in

SWIZ:GFP-OE. LB, left border; *ZmUbi* prom, maize ubiquitin promoter; Hyg, hygromycin phosphotransferase gene; NOS, nopaline synthase terminator; RB, right border. ns: $p > 0.05$, : *: $p < 0.05$.

Supplemental Figure 2. Network analysis of differential gene expression paths and enriched GO terms. (A) Path determinations from iDREM time course analysis. Each line represents a set of genes with similar expression level patterns over the time course relative to time 0, pre-touch. (B) Heatmap of selected GO term enrichment of genes from iDREM path analysis. Color indicates *q*-value score, with a cutoff of 0.1. Terms without a colored block are not significantly enriched in that path.

Supplemental Figure 3. Thigmomatic, an automated system to administer touch stimulus. (A) Overview of Thigmomatic inside a Percival PGC-15 growth chamber showing linear rail based frame (1), gantry carts (2), NEMA17 stepper motor (3), 12V 18W AC/DC power supply (4), and Raspberry Pi 3b microcomputer (5). (B) Thigmomatic making contact with a *Brachypodium distachyon* plant.

Supplemental Figure 4. Brachypodium distachyon displays classic thigmomorphogenic phenotypes. One-week-old wildtype plants were treated with touch stimulus every 90 min. (A) Left to right, plants that experienced no stress, two weeks stress, three weeks stress and were then allowed to recover, imaged one week after the end of treatment (B) height, (C) aboveground non-grain biomass weight, and (D) branch number were measured at senescence. Significance denoted by compact letter display reflecting Tukey HSD adjusted p-values < 0.05. (E) Transverse sections of the peduncle or third internode were taken from control, 2 week stressed, and 3 week stressed plants and stained with phloroglucinol-HCl. (F) Quantification of interfascicular fiber wall thickness. Scale bar = 100 μm. n = 3 plants per treatment.

Supplemental Figure 5. Biomass and branching in SWIZ-OE under touch treatment shows no difference from wildtype. Wildtype and SWIZ-OE plants were placed under control conditions or received two weeks of mechanical stress every 90 min. After senescence, branch number (A) and aboveground biomass weight (B) were quantified. Significant differences were not observed following ANOVA and Tukey HSD testing.

Supplemental Figure 6. Brachypodium distachyon cis-regulatory sequences most overrepresented at each time course after touching. Each nucleotide sequence is a position probability matrix motif derived from DNA-affinity purification sequencing and identified as enriched under different time courses. The height of the letter at each position is proportional to the probability of a given nucleotide.

Supplemental Figure 7. Method of root touch treatment. A blunt probe formed from a glass Pasteur pipette was used to gently tap on the root five times in areas similar to those indicated by

the orange arrows.

Supplemental File 1. Gene names and amino acid sequences used in the SWIZ bZIP Group I phylogenetic analysis.

ACCESSION NUMBERS

AtbZIP18 (At2g40620), AtbZIP29 (At4g38900), AtbZIP52 (At1g06850), AtTCH1/AtCaM2 (At2g41110), AtTCH2/AtCML24 (At5g37770), AtTCH3/CML12 (At2g41100), AtTCH4/AtXTH22 (At5g57560), CAD1 (Bradi3g17920), CESA4 (Bradi4g28350), COMT6 (Bradi3g16530), CSLF6 (Bradi3g16307), GA2ox3 (Bradi2g50280), SWAM3/MYB44 (Bradi1g30252), NAC35 (Bradi2g28020), NtRSGa (Niben101Scf01150g00005), NtRSGb (Niben101Scf02191g00014), SWIZ (Bradi1g17700), VIP1 (At1g43700).

ACKNOWLEDGEMENTS

This work was supported by the Office of Science, Biological and Environmental Research, Department of Energy (DE-FG02-08ER64700DE and DE-SC0006641) and The National Science Foundation Division of Integrative Organismal Systems (NSF IOS-1558072) to S.P.H.. The work conducted by the US DOE Joint Genome Institute is supported by the Office of Science of the US Department of Energy under Contract no. DE-AC02-05CH11231. The microscopy data was gathered in the Light Microscopy Facility and Nikon Center of Excellence at the Institute for Applied Life Sciences, UMass Amherst with support from the Massachusetts Life Sciences Center.

Table 1. The count of differentially expressed genes relative to untouched wildtype plants that were SWIZ DAP-seq targets in either the promoter or gene body regions.

Time after touch	Promoter		Gene body	
	Up	Down	Up	Down
(min)	percent (count)			
0	42.0 (103)	58.0 (142)	48.0 (286)	52.0 (310)
10	57.0 (73)	43.0 (55)	53.0 (167)	47.0 (148)
30	59.4 (79)	40.6 (54)	41.2 (136)	58.8 (194)

60	64.2 (77)	35.8 (43)	45.7 (128)	54.3 (152)

FIGURE LEGENDS

Figure 1. SWIZ is a Group I bZIP highly expressed in maturing stem and root. (A) *SWIZ* transcript abundance in *Brachypodium distachyon* leaf, root, and stem tissue measured by microarray. Mean +/- standard deviation of three biological replicates. (B) Phylogeny analysis of amino acid sequences from *B. distachyon* (green), *Oryza sativa* (blue), *Arabidopsis thaliana* (red), *Nicotiana tabacum* (orange) shows *SWIZ* (black dot). The phylogeny was reconstructed using maximum likelihood analysis with a bootstrap resampling value of 1000. The numbers labeled on the branches are the posterior probability to support each clade. The protein sequences, full locus IDs, and plant species with genome source are provided in Supplemental File 1.

Figure 2. SWIZ translocates to the nucleus in response to mechanical stimulus, specifically in regions directly stimulated. (A) Image of *SWIZ:GFP-OE* and *GFP-OE* roots prior to stimulus and 30 min post stimulus. Roots were observed immediately following mechanical perturbation. (B) Quantification of nuclear signal in control (purple) and touched (teal) conditions for *GFP-OE* (left) and *SWIZ:GFP-OE* (right). n = 14-20 nuclei. (C) SWIZ translocation occured in the local area of the stimulus. At 30 min, stimulus was applied to an upper region of the root, while at 120 min it was applied to a lower region approximately 3 cm below. n = 109, 184 nuclei respectively for upper and lower regions. (D) *SWIZ:GFP-OE* roots were imaged by confocal microscopy with stimulus applied in the field of view at 0, 90, and 180 min. n = 126 nuclei. (B-D) Images were taken every 2 min. Nuclear GFP signal was quantified in selected nuclei at each time point. The average nuclear GFP signal is represented by the line with error bars indicating standard error of the mean.

Figure 3. Transcriptome analysis of touch response in *Brachypodium distachyon* roots. (A) Root tissue was sampled just prior to touch (t = 0), and at 10, 30, and 60 min following touch treatment in wildtype and *SWIZ-OE*. (B) Principal component analysis of gene expression across samples shows the greatest difference corresponding to genotype and the second greatest corresponding to time after touch. (C) Canonical, as well as novel touch responsive genes are upregulated in *B. distachyon* following touch. Closest orthologs of the *Arabidopsis thaliana TOUCH* genes encoding calmodulin-like (CML) and xyloglucan endo-transglycosylase/hydrolases (XTH) are upregulated following touch, as are previously unreported members of the glycosyl hydrolase 17 (GH17) family. Full list of gene expression for *TOUCH* and glycoside hydrolases defined by Tyler et al. (2010) in Supplemental Tables 5, 6,and 7. Significance denoted by * reflecting $q < 0.1$ compared to expression at t = 0, with q-values representing Wald test p-values adjusted for false discovery rate.

Figure 4. Gene expression analysis of cell wall related genes. Log fold-change of gene expression measured by RNA-seq in wildtype and *SWIZ-OE*, presented as relative to wildtype

773 expression at time 0, pre-touch. Bar color indicates class of cell wall gene. Error bars indicate
774 standard deviation of three biological replicates. Significance denoted by * reflecting $q < 0.1$
775 compared to wildtype expression at $t = 0$, with q-values representing Wald test p-values adjusted
776 for false discovery rate. Legend abbreviations: BAHD, BAHD (BEAT, AHCT, HCBT, and
777 DAT) acyltransferases; CESA, cellulose synthase; MLG, mixed-linkage glucans.
778
779 **Figure 5. DNA affinity purification sequencing to determine SWIZ binding sites.** (A) Top
780 two most statistically enriched sequence motifs in SWIZ binding sites. (B) Distribution of
781 binding sites across genomic features, relative to primary transcripts of the *Brachypodium*
782 *distachyon* annotation v 3.1. (C) Relative distribution of binding sites centered on the
783 transcriptional start site (TSS, blue dashed line), transcriptional termination site (TTS, red dashed
784 line) represents the average length of all annotated transcripts, approximately 4.5 kb away from
785 the TSS. (D) Path determinations from iDREM time course analysis of differentially expressed
786 genes that also have DAP-seq binding sites. Each line represents a set of genes with similar
787 expression level patterns over the time course relative to time 0, pre-touch.
788
789 **Figure 6. SWIZ binding targets differentially expressed in response to touch and *SWIZ-OE*.**
790 Gene expression over time of selected genes with SWIZ binding sites. Line graphs are the
791 average transcript abundance of three biological replicates for each time point. Binding site
792 determined as peaks of sequence alignment. Scale bar unit is bases. Direction of transcription is
793 shown with arrows on the gene model, 5' and 3' UTRs are depicted by narrowed rectangles on
794 the gene model.
795
796 **Figure 7. Sequence motifs enriched in the *cis*-regulatory regions of touch responsive**
797 ***Brachypodium distachyon* genes.** Negative log *p*-values for *cis*-elements, known and not known
798 to be touch responsive. RSRE - Rapid Stress Response Element, FAR1 - FAR-RED impaired
799 response1, GRF - Growth Regulating Factor, VNS - VND, NST/SND, SMB.
800
801 **Figure 8. *SWIZ-OE* roots are shorter than wildtype with no significant difference in**
802 **straightness in response to direct touch.** Wildtype and *SWIZ-OE* seedlings grown on plates
803 under control (A) or touched (B) conditions for five days. Touched plants were probed with a
804 pipette tip twice a day. (C) Quantification of root length in control and touched conditions.
805 Significance denoted by compact letter display reflecting Tukey HSD adjusted *p* values < 0.05.
806 (D) Quantification of root straightness in control and touch conditions. Significance denoted by *
807 reflecting Wilcoxon sign-ranked test for non-parametric data with *p*-value < 0.05, ns = not
808 significant. Scale bar = 1 cm.
809
810 **Figure 9. Wildtype roots shorten with increasing plate angle, while *SWIZ-OE* roots are**
811 **consistently short, with no significant difference in straightness.** Wildtype and *SWIZ-OE*
812 seedlings grown on plates at (A) 10°, 20°, 30°, and (B) 40° incline from vertical. (C)
813 Quantification of root length. (D) Quantification of primary root straightness. Significance
814 denoted by compact letter display reflecting Tukey HSD adjusted *p*-values < 0.05. Scale bar = 1
815 cm.
816
817 **Figure 10. *SWIZ-OE* marginally enhanced thigmomorphogenic response in stems.** Wildtype

and *SWIZ-OE* plants were placed under control conditions or received two weeks of mechanical stress every 90 min. (A) Quantification of main stem height at senescence. (B) Quantification of interfascicular fiber wall thickness in transverse cross sections of the peduncle. n = 4 to 6 plants per genotype, per treatment. (C) Representative cross sections stained with phloroglucinol-HCl. Scale bar = 100 µm. Significance denoted by compact letter display reflecting Tukey HSD adjuste*d p*-values < 0.05.

REFERENCES

Altartouri B, Bidhendi AJ, Tani T, Suzuki J, Conrad C, Chebli Y, Liu N, Karunakaran C, Scarcelli G, Geitmann A (2019) Pectin chemistry and cellulose crystallinity govern pavement cell morphogenesis in a multi-step mechanism. Plant Physiol **181**: 127–141

Andrews S (2010) FastQC: a quality control tool for high throughput sequence data. http://www.bioinformatics.babraham.ac.uk/projects/fastqc:

Bidhendi AJ, Altartouri B, Gosselin FP, Geitmann A (2019) Mechanical stress initiates and sustains the morphogenesis of wavy leaf epidermal cells. Cell Rep **28**: 1237–1250.e6

Bidhendi AJ, Geitmann A (2018) Finite element modeling of shape changes in plant cells. Plant Physiol **176**: 41–56

Biro RL, Hunt ER, Erner Y, Jaffe MJ (1980) Thigmomorphogenesis: changes in cell division and elongation in the internodes of mechanically-perturbed or ethrel-treated bean plants. Ann Bot **45**: 655–664

Börnke F, Rocksch T (2018) Thigmomorphogenesis – Control of plant growth by mechanical stimulation. Sci Hortic **234**: 344–353

Braam J (2004) In touch: plant responses to mechanical stimuli. New Phytol **165**: 373–389

Braam J, Davis RW (1990) Rain-, wind-, and touch-induced expression of calmodulin and calmodulin-related genes in Arabidopsis. Cell **60**: 357–364

Chehab EW, Eich E, Braam J (2009) Thigmomorphogenesis: a complex plant response to mechano-stimulation. J Exp Bot **60**: 43–56

Coomey JH, Sibout R, Hazen SP (2020) Grass secondary cell walls, *Brachypodium distachyon* as a model for discovery. New Phytol **227**: 1709–1724

Coutand C, Martin L, Leblanc-Fournier N, Decourteix M, Julien J-L, Moulia B (2009) Strain mechanosensing quantitatively controls diameter growth and PtaZFP2 gene expression in poplar. Plant Physiol **151**: 223–232

Deppmann CD, Acharya A, Rishi V, Wobbes B, Smeekens S, Taparowsky EJ, Vinson C (2004) Dimerization specificity of all 67 B-ZIP motifs in *Arabidopsis thaliana*: a

853 comparison to *Homo sapiens* B-ZIP motifs. Nucleic Acids Res **32**: 3435–3445

854 **Ding J, Hagood JS, Ambalavanan N, Kaminski N, Bar-Joseph Z** (2018) iDREM: Interactive
855 visualization of dynamic regulatory networks. PLoS Comput Biol **14**: e1006019

856 **Doherty CJ, Van Buskirk HA, Myers SJ, Thomashow MF** (2009) Roles for Arabidopsis
857 CAMTA transcription factors in cold-regulated gene expression and freezing tolerance.
858 Plant Cell **21**: 972–984

859 **Dröge-Laser W, Snoek BL, Snel B, Weiste C** (2018) The Arabidopsis bZIP transcription factor
860 family-an update. Curr Opin Plant Biol **45**: 36–49

861 **Ehlert A, Weltmeier F, Wang X, Mayer CS, Smeekens S, Vicente-Carbajosa J, Dröge-**
862 **Laser W** (2006) Two-hybrid protein-protein interaction analysis in Arabidopsis protoplasts:
863 establishment of a heterodimerization map of group C and group S bZIP transcription
864 factors. Plant J **46**: 890–900

865 **Fernández-Calvo P, Chini A, Fernández-Barbero G, Chico J-M, Gimenez-Ibanez S,**
866 **Geerinck J, Eeckhout D, Schweizer F, Godoy M, Franco-Zorrilla JM, et al** (2011) The
867 Arabidopsis bHLH transcription factors MYC3 and MYC4 are targets of JAZ repressors
868 and act additively with MYC2 in the activation of jasmonate responses. Plant Cell **23**: 701–
869 715

870 **Fukazawa J, Nakata M, Ito T, Matsushita A, Yamaguchi S, Takahashi Y** (2011) bZIP
871 transcription factor RSG controls the feedback regulation of NtGA20ox1 via intracellular
872 localization and epigenetic mechanism. Plant Signal Behav **6**: 26–28

873 **Fukazawa J, Nakata M, Ito T, Yamaguchi S, Takahashi Y** (2010) The transcription factor
874 RSG regulates negative feedback of NtGA20ox1 encoding GA 20-oxidase. Plant J **62**:
875 1035–1045

876 **Fukazawa J, Sakai T, Ishida S, Yamaguchi I, Kamiya Y, Takahashi Y** (2000) Repression of
877 shoot growth, a bZIP transcriptional activator, regulates cell elongation by controlling the
878 level of gibberellins. Plant Cell **12**: 901–915

879 **Gibalová A, Steinbachová L, Hafidh S, Bláhová V, Gadiou Z, Michailidis C, Műller K,**
880 **Pleskot R, Dupľáková N, Honys D** (2017) Characterization of pollen-expressed bZIP
881 protein interactions and the role of ATbZIP18 in the male gametophyte. Plant Reprod **30**:
882 1–17

883 **Gladala-Kostarz A, Doonan JH, Bosch M** (2020) Mechanical stimulation in *Brachypodium*
884 *distachyon*: implications for fitness, productivity and cell wall properties. Plant Cell
885 Environ **43**: 1314–1330

886 **Grigoryan G, Keating AE** (2006) Structure-based prediction of bZIP partnering specificity. J
887 Mol Biol **355**: 1125–1142

888 **Hamant O, Heisler MG, Jönsson H, Krupinski P, Uyttewaal M, Bokov P, Corson F, Sahlin**

889 **P, Boudaoud A, Meyerowitz EM, et al** (2008) Developmental patterning by mechanical
890 signals in Arabidopsis. Science **322**: 1650–1655

891 **Handakumbura P, Matos D, Osmont K, Harrington M, Heo K, Kafle K, Kim S, Baskin T,**
892 **Hazen S** (2013) Perturbation of *Brachypodium distachyon CELLULOSE SYNTHASE A4* or
893 *7* results in abnormal cell walls. BMC Plant Biol **13**: 131

894 **Handakumbura PP, Brow K, Whitney IP, Zhao K, Sanguinet KA, Lee SJ, Olins J,**
895 **Romero-Gamboa SP, Harrington MJ, Bascom CJ, et al** (2018) *SECONDARY WALL*
896 *ASSOCIATED MYB1* is a positive regulator of secondary cell wall thickening in
897 *Brachypodium distachyon* and is not found in the Brassicaceae. Plant J **96**: 485–699

898 **Heinz S, Benner C, Spann N, Bertolino E, Lin YC, Laslo P, Cheng JX, Murre C, Singh H,**
899 **Glass CK** (2010) Simple combinations of lineage-determining transcription factors prime
900 *cis*-regulatory elements required for macrophage and B cell identities. Mol Cell **38**: 576–
901 589

902 **Igarashi D, Ishida S, Fukazawa J, Takahashi Y** (2001) 14-3-3 proteins regulate intracellular
903 localization of the bZIP transcriptional activator RSG. Plant Cell **13**: 2483–2497

904 **Iida H** (2014) Mugifumi, a beneficial farm work of adding mechanical stress by treading to
905 wheat and barley seedlings. Front Plant Sci **5**: 453

906 **Ishida S, Fukazawa J, Yuasa T, Takahashi Y** (2004) Involvement of 14-3-3 signaling protein
907 binding in the functional regulation of the transcriptional activator REPRESSION OF
908 SHOOT GROWTH by gibberellins. Plant Cell **16**: 2641–2651

909 **Ishida S, Yuasa T, Nakata M, Takahashi Y** (2008) A tobacco calcium-dependent protein
910 kinase, CDPK1, regulates the transcription factor REPRESSION OF SHOOT GROWTH in
911 response to gibberellins. Plant Cell **20**: 3273–3288

912 **Ito T, Ishida S, Oe S, Fukazawa J, Takahashi Y** (2017) Autophosphorylation affects substrate-
913 binding affinity of tobacco Ca2+-dependent protein kinase1. Plant Physiol **174**: 2457–2468

914 **Ito T, Nakata M, Fukazawa J, Ishida S, Takahashi Y** (2014) Scaffold function of Ca2+-
915 dependent protein kinase: tobacco Ca2+-DEPENDENT PROTEIN KINASE1 transfers 14-
916 3-3 to the substrate REPRESSION OF SHOOT GROWTH after phosphorylation. Plant
917 Physiol **165**: 1737–1750

918 **Jaffe MJ** (1973) Thigmomorphogenesis: The response of plant growth and development to
919 mechanical stimulation : With special reference to Bryonia dioica. Planta **114**: 143–157

920 **Jaffe MJ, Biro R, Bridle K** (1980) Thigmomorphogenesis: Calibration of the parameters of the
921 sensory function in beans. Physiol Plant **49**: 410–416

922 **Jakoby M, Weisshaar B, Dröge-Laser W, Vicente-Carbajosa J, Tiedemann J, Kroj T,**
923 **Parcy F, bZIP Research Group** (2002) bZIP transcription factors in Arabidopsis. Trends
924 Plant Sci **7**: 106–111

925 **Katoh K, Rozewicki J, Yamada KD** (2019) MAFFT online service: multiple sequence
926 alignment, interactive sequence choice and visualization. Brief Bioinform **20**: 1160–1166

927 **Kim D, Langmead B, Salzberg SL** (2015) HISAT: a fast spliced aligner with low memory
928 requirements. Nat Methods **12**: 357

929 **Kim W-C, Ko J-H, Han K-H** (2012) Identification of a *cis*-acting regulatory motif recognized
930 by MYB46, a master transcriptional regulator of secondary wall biosynthesis. Plant Mol
931 Biol **78**: 489–501

932 **Leblanc-Fournier N, Martin L, Lenne C, Decourteix M** (2014) To respond or not to respond,
933 the recurring question in plant mechanosensitivity. Front Plant Sci **5**: 401

934 **Lee D, Polisensky DH, Braam J** (2005) Genome-wide identification of touch- and darkness-
935 regulated Arabidopsis genes: a focus on calmodulin-like and XTH genes. New Phytol **165**:
936 429–444

937 **Lee H-J, Kim H-S, Park JM, Cho HS, Jeon JH** (2019) PIN-mediated polar auxin transport
938 facilitates root obstacle avoidance. New Phytol. doi: 10.1111/nph.16076

939 **Lee TG, Jang CS, Kim JY, Kim DS, Park JH, Kim DY, Seo YW** (2006) A Myb transcription
940 factor (TaMyb1) from wheat roots is expressed during hypoxia: roles in response to the
941 oxygen concentration in root environment and abiotic stresses. Physiol Plant **129**: 375–385

942 **Li H, Handsaker B, Wysoker A, Fennell T, Ruan J, Homer N, Marth G, Abecasis G,**
943 **Durbin R, 1000 Genome Project Data Processing Subgroup** (2009) The Sequence
944 Alignment/Map format and SAMtools. Bioinformatics **25**: 2078–2079

945 **Liu R, Finlayson SA** (2019) Sorghum tiller bud growth is repressed by contact with the
946 overlying leaf. Plant Cell Environ **42**: 2120–2132

947 **Liu X, Chu Z** (2015) Genome-wide evolutionary characterization and analysis of bZIP
948 transcription factors and their expression profiles in response to multiple abiotic stresses in
949 Brachypodium distachyon. BMC Genomics **16**: 227

950 **Lobet G, Pagès L, Draye X** (2011) A novel image-analysis toolbox enabling quantitative
951 analysis of root system architecture. Plant Physiol **157**: 29–39

952 **Lourenço TF, Serra TS, Cordeiro AM, Swanson SJ, Gilroy S, Saibo NJM, Oliveira MM**
953 (2015) The Rice E3-Ubiquitin Ligase HIGH EXPRESSION OF OSMOTICALLY
954 RESPONSIVE GENE1 Modulates the Expression of ROOT MEANDER CURLING, a
955 Gene Involved in Root Mechanosensing, through the Interaction with Two ETHYLENE-
956 RESPONSE FACTOR Transcription Factors. Plant Physiol **169**: 2275–2287

957 **Love MI, Huber W, Anders S** (2014) Moderated estimation of fold change and dispersion for
958 RNA-seq data with DESeq2. Genome Biol **15**: 550

959 **MacKinnon KJ-M, Cole BJ, Yu C, Coomey JH, Hartwick NT, Remigereau M-S, Duffy T,**

960 **Michael TP, Kay SA, Hazen SP** (2020) Changes in ambient temperature are the prevailing
961 cue in determining *Brachypodium distachyon* diurnal gene regulation. New Phytol **227**:
962 1649–1667

963 **Martin L, Leblanc-Fournier N, Julien J-L, Moulia B, Coutand C** (2010) Acclimation
964 kinetics of physiological and molecular responses of plants to multiple mechanical loadings.
965 J Exp Bot **61**: 2403–2412

966 **Matos DA, Whitney IP, Harrington MJ, Hazen SP** (2013) Cell walls and the developmental
967 anatomy of the *Brachypodium distachyon* stem internode. PLoS One **8**: e80640

968 **McCahill IW, Hazen SP** (2019) Regulation of cell wall thickening by a medley of mechanisms.
969 Trends Plant Sci **24**: 853–866

970 **Monshausen GB, Bibikova TN, Weisenseel MH, Gilroy S** (2009) Ca2+ regulates reactive
971 oxygen species production and pH during mechanosensing in Arabidopsis roots. Plant Cell
972 **21**: 2341–2356

973 **Moore BM, Lee YS, Wang P, Azodi C, Grotewold E, Shiu S-H** (2022) Modeling temporal
974 and hormonal regulation of plant transcriptional response to wounding. Plant Cell **34**: 867–
975 888

976 **Moulia B, Coutand C, Julien J-L** (2015) Mechanosensitive control of plant growth: bearing the
977 load, sensing, transducing, and responding. Front Plant Sci **6**: 52

978 **Nam BE, Park Y-J, Gil K-E, Kim J-H, Kim JG, Park C-M** (2020) Auxin mediates the touch-
979 induced mechanical stimulation of adventitious root formation under windy conditions in
980 Brachypodium distachyon. BMC Plant Biol **20**: 335

981 **Niez B, Dlouha J, Moulia B, Badel E** (2019) Water-stressed or not, the mechanical acclimation
982 is a priority requirement for trees. Trees **33**: 279–291

983 **Ohtani M, Nishikubo N, Xu B, Yamaguchi M, Mitsuda N, Goué N, Shi F, Ohme-Takagi M,**
984 **Demura T** (2011) A NAC domain protein family contributing to the regulation of wood
985 formation in poplar. Plant J **67**: 499–512

986 **Olins JR, Lin L, Lee SJ, Trabucco GM, MacKinnon KJM, Hazen SP** (2018) Secondary wall
987 regulating NACs differentially bind at the promoter at a *CELLULOSE SYNTHASE A4* cis-
988 eQTL. Front Plant Sci **9**: 1895

989 **Oliva M, Dunand C** (2007) Waving and skewing: how gravity and the surface of growth media
990 affect root development in Arabidopsis. New Phytol **176**: 37–43

991 **O'Malley RC, Huang S-SC, Song L, Lewsey MG, Bartlett A, Nery JR, Galli M, Gallavotti**
992 **A, Ecker JR** (2016) Cistrome and epicistrome features shape the regulatory DNA
993 landscape. Cell **165**: 1280–1292

994 **Pertea M, Pertea GM, Antonescu CM, Chang T-C, Mendell JT, Salzberg SL** (2015)

StringTie enables improved reconstruction of a transcriptome from RNA-seq reads. Nat Biotechnol **33**: 290–295

Pitzschke A, Djamei A, Teige M, Hirt H (2009) VIP1 response elements mediate mitogen-activated protein kinase 3-induced stress gene expression. Proc Natl Acad Sci U S A **106**: 18414–18419

Polisensky DH, Braam J (1996) Cold-shock regulation of the Arabidopsis TCH genes and the effects of modulating intracellular calcium levels. Plant Physiol **111**: 1271–1279

Pomiès L, Decourteix M, Franchel J, Moulia B, Leblanc-Fournier N (2017) Poplar stem transcriptome is massively remodelled in response to single or repeated mechanical stimuli. BMC Genomics **18**: 300

Raudvere U, Kolberg L, Kuzmin I, Arak T, Adler P, Peterson H, Vilo J (2019) g:Profiler: a web server for functional enrichment analysis and conversions of gene lists. Nucleic Acids Res **47**: W191–W198

Ringli C, Keller B (1998) Specific interaction of the tomato bZIP transcription factor VSF-1 with a non-palindromic DNA sequence that controls vascular gene expression. Plant Mol Biol **37**: 977–988

Roignant J, Badel É, Leblanc-Fournier N, Brunel-Michac N, Ruelle J, Moulia B, Decourteix M (2018) Feeling stretched or compressed? The multiple mechanosensitive responses of wood formation to bending. Ann Bot **121**: 1151–1161

Rushton PJ, Reinstädler A, Lipka V, Lippok B, Somssich IE (2002) Synthetic plant promoters containing defined regulatory elements provide novel insights into pathogen- and wound-induced signaling. Plant Cell **14**: 749–762

Schütze K, Harter K, Chaban C (2008) Post-translational regulation of plant bZIP factors. Trends Plant Sci **13**: 247–255

Shah L, Yahya M, Shah SMA, Nadeem M, Ali A, Ali A, Wang J, Riaz MW, Rehman S, Wu W, et al (2019) Improving lodging resistance: using wheat and rice as classical examples. Int J Mol Sci. doi: 10.3390/ijms20174211

Sibout R, Proost S, Hansen BO, Vaid N, Giorgi FM, Ho-Yue-Kuang S, Legée F, Cézart L, Bouchabké-Coussa O, Soulhat C, et al (2017) Expression atlas and comparative coexpression network analyses reveal important genes involved in the formation of lignified cell wall in *Brachypodium distachyon*. New Phytol **215**: 1009–1025

Swanson SJ, Barker R, Ye Y, Gilroy S (2015) Evaluating mechano-transduction and touch responses in plant roots. Methods Mol Biol **1309**: 143–150

Szczegielniak J, Borkiewicz L, Szurmak B, Lewandowska-Gnatowska E, Statkiewicz M, Klimecka M, Cieśla J, Muszyńska G (2012) Maize calcium-dependent protein kinase (ZmCPK11): local and systemic response to wounding, regulation by touch and components

of jasmonate signaling. Physiol Plant **146**: 1–14

Trabucco GM, Matos DA, Lee SJ, Saathoff A, Priest H, Mockler TC, Sarath G, Hazen SP (2013) Functional characterization of cinnamyl alcohol dehydrogenase and caffeic acid *O*-methyltransferase in *Brachypodium distachyon*. BMC Biotechnol **13**: 61

Trifinopoulos J, Nguyen L-T, von Haeseler A, Minh BQ (2016) W-IQ-TREE: a fast online phylogenetic tool for maximum likelihood analysis. Nucleic Acids Res **44**: W232–W235

Tsugama D, Liu S, Fujino K, Takano T (2018) Calcium signalling regulates the functions of the bZIP protein VIP1 in touch responses in *Arabidopsis thaliana*. Ann Bot **122**: 1219–1229

Tsugama D, Liu S, Takano T (2012) A bZIP protein, VIP1, is a regulator of osmosensory signaling in Arabidopsis. Plant Physiol **159**: 144–155

Tsugama D, Liu S, Takano T (2016) The bZIP protein VIP1 Is involved in touch responses in Arabidopsis roots. Plant Physiol **171**: 1355–1365

Tsugama D, Liu S, Takano T (2014) Analysis of functions of VIP1 and its close homologs in osmosensory responses of *Arabidopsis thaliana*. PLoS One **9**: e103930

Tyler L, Bragg JN, Wu J, Yang X, Tuskan GA, Vogel JP (2010) Annotation and comparative analysis of the glycoside hydrolase genes in *Brachypodium distachyon*. BMC Genomics **11**: 600

Uyttewaal M, Burian A, Alim K, Landrein B, Borowska-Wykręt D, Dedieu A, Peaucelle A, Ludynia M, Traas J, Boudaoud A, et al (2012) Mechanical stress acts via katanin to amplify differences in growth rate between adjacent cells in Arabidopsis. Cell **149**: 439–451

Valdivia ER, Herrera MT, Gianzo C, Fidalgo J, Revilla G, Zarra I, Sampedro J (2013) Regulation of secondary wall synthesis and cell death by NAC transcription factors in the monocot *Brachypodium distachyon*. J Exp Bot **64**: 1333–1343

Van Leene J, Blomme J, Kulkarni SR, Cannoot B, De Winne N, Eeckhout D, Persiau G, Van De Slijke E, Vercruysse L, Vanden Bossche R, et al (2016) Functional characterization of the Arabidopsis transcription factor bZIP29 reveals its role in leaf and root development. J Exp Bot **67**: 5825–5840

Van Moerkercke A, Duncan O, Zander M, Šimura J, Broda M, Vanden Bossche R, Lewsey MG, Lama S, Singh KB, Ljung K, et al (2019) A MYC2/MYC3/MYC4-dependent transcription factor network regulates water spray-responsive gene expression and jasmonate levels. Proc Natl Acad Sci U S A **116**: 23345–23356

Walley J, Coughlan S, Hudson ME, Covington MF, Kaspi R, Banu G, Harmer SL, Dehesh K (2007) Mechanical stress induces biotic and abiotic stress responses via a novel cis-element. PLoS Genet **3**: 1800–1812

Weltmeier F, Ehlert A, Mayer CS, Dietrich K, Wang X, Schütze K, Alonso R, Harter K,

Vicente-Carbajosa J, Dröge-Laser W (2006) Combinatorial control of Arabidopsis proline dehydrogenase transcription by specific heterodimerisation of bZIP transcription factors. EMBO J **25**: 3133–3143

Yin Y, Zhu Q, Dai S, Lamb C, Beachy RN (1997) RF2a, a bZIP transcriptional activator of the phloem-specific rice tungro bacilliform virus promoter, functions in vascular development. EMBO J **16**: 5247–5259

Zha G, Wang B, Liu J, Yan J, Zhu L, Yang X (2016) Mechanical touch responses of Arabidopsis TCH1-3 mutant roots on inclined hard-agar surface. International Agrophysics **30**: 65

Zhong R, Lee C, McCarthy RL, Reeves CK, Jones EG, Ye Z-H (2011) Transcriptional activation of secondary wall biosynthesis by rice and maize NAC and MYB transcription factors. Plant Cell Physiol **52**: 1856–1871

Zhong R, Ye Z-H (2012) MYB46 and MYB83 bind to the SMRE sites and directly activate a suite of transcription factors and secondary wall biosynthetic genes. Plant Cell Physiol **53**: 368–380

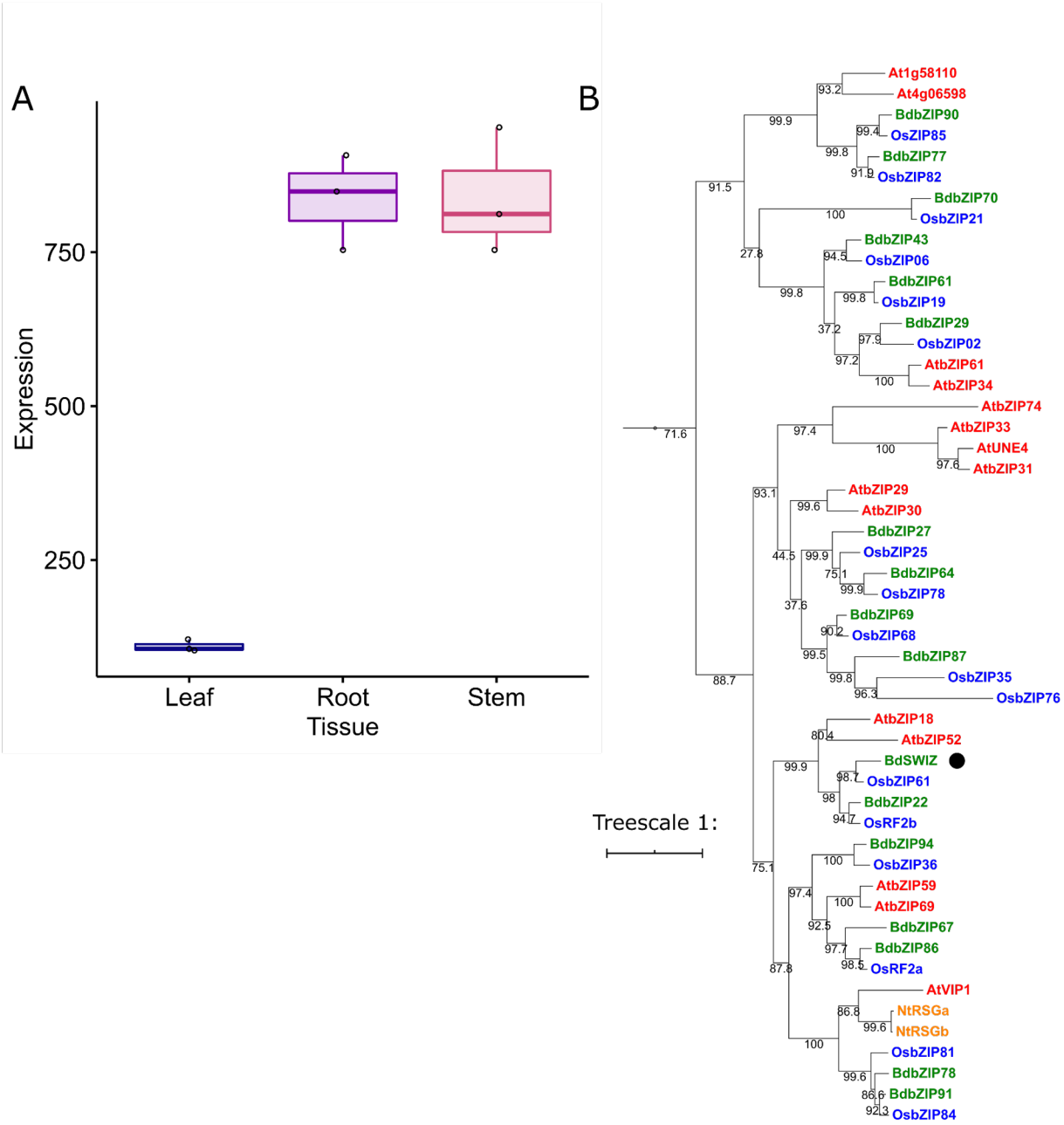

Figure 1. SWIZ is a Group I bZIP highly expressed in maturing stem and root. (A) *SWIZ* transcript abundance in *Brachypodium distachyon* leaf, root, and stem tissue measured by microarray. Mean +/- standard deviation of three biological replicates. (B) Phylogeny analysis of amino acid sequences from *B. distachyon* (green), *Oryza sativa* (blue), *Arabidopsis thaliana* (red), *Nicotiana tabacum* (orange) shows *SWIZ* (black dot). The phylogeny was reconstructed using maximum likelihood analysis with a bootstrap resampling value of 1000. The numbers labeled on the branches are the posterior probability to support each clade. The protein sequences, full locus IDs, and plant species with genome source are provided in Supplemental File 1.

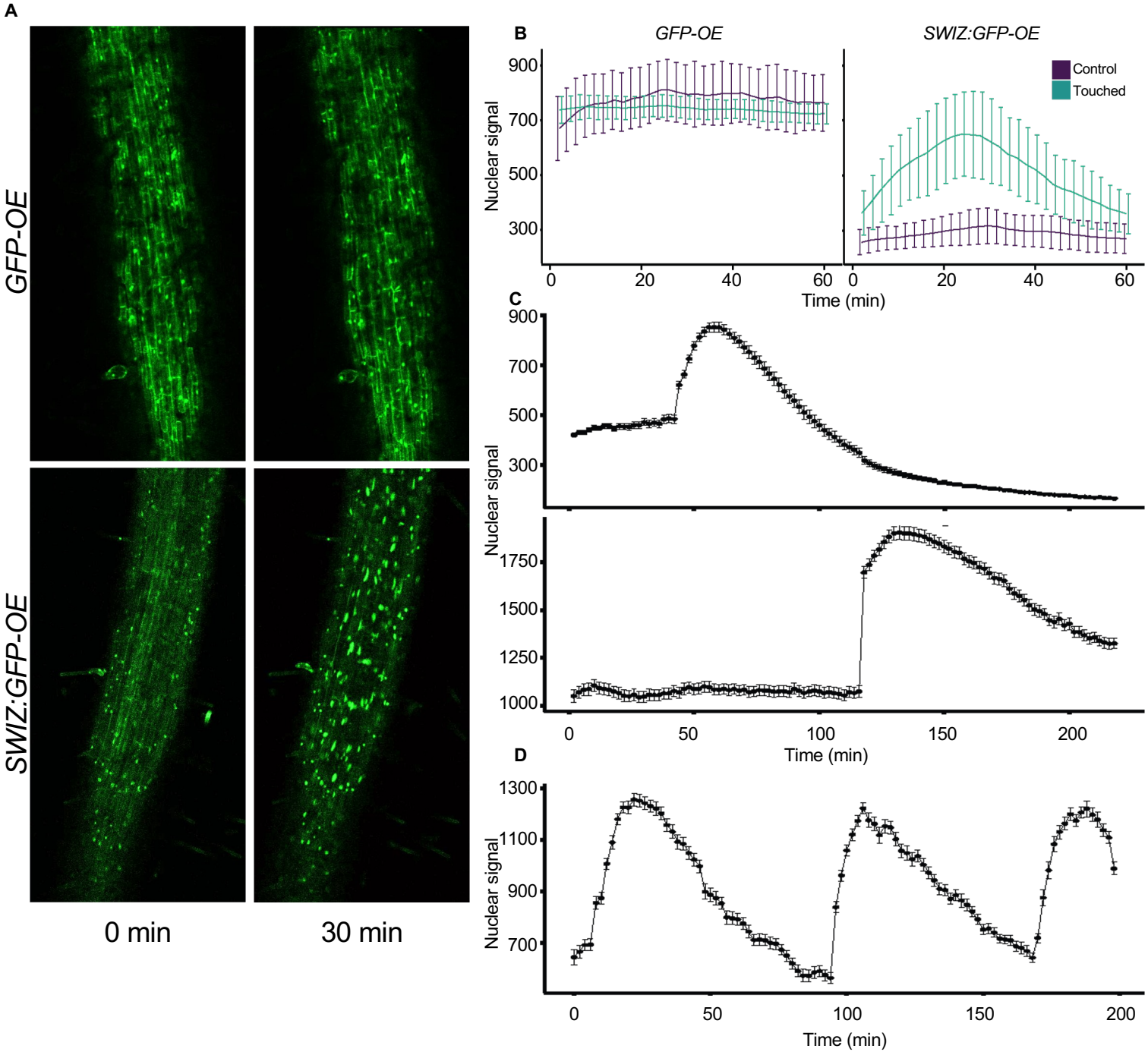

Figure 2. SWIZ translocates to the nucleus in response to mechanical stimulus, specifically in regions directly stimulated. (A) Image of *SWIZ:GFP-OE* and *GFP-OE* roots prior to stimulus and 30 min post stimulus. Roots were observed immediately following mechanical perturbation. (B) Quantification of nuclear signal in control (purple) and touched (teal) conditions for *GFP-OE* (left) and *SWIZ:GFP-OE* (right). n = 14-20 nuclei. (C) SWIZ translocation occured in the local area of the stimulus. At 30 min, stimulus was applied to an upper region of the root, while at 120 min it was applied to a lower region approximately 3 cm below. n = 109, 184 nuclei respectively for upper and lower regions. (D) *SWIZ:GFP-OE* roots were imaged by confocal microscopy with stimulus applied in the field of view at 0, 90, and 180 min. n = 126 nuclei. (B-D) Images were taken every 2 min. Nuclear GFP signal was quantified in selected nuclei at each time point. The average nuclear GFP signal is represented by the line with error bars indicating standard error of the mean.

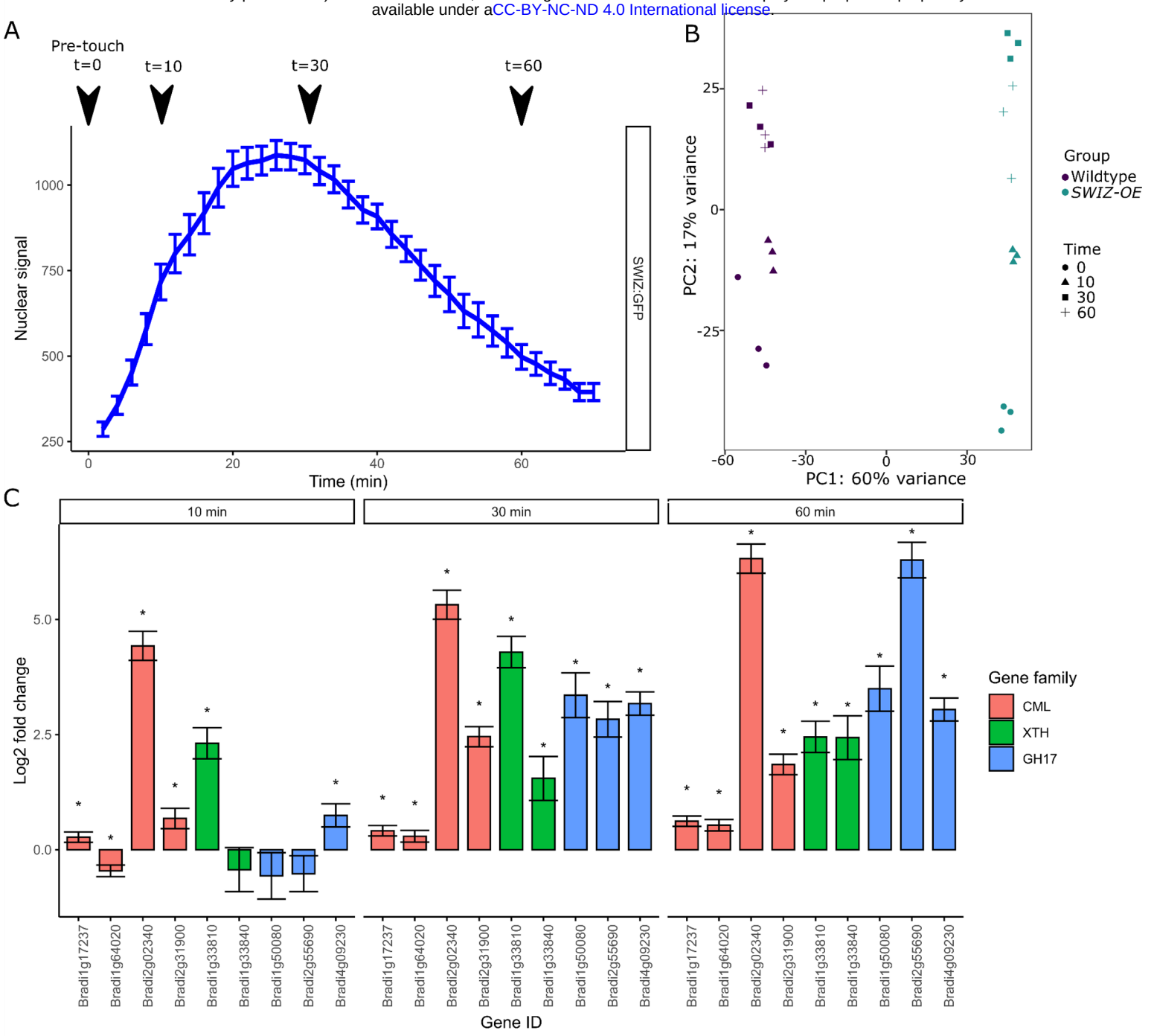

Figure 3. Transcriptome analysis of touch response in *Brachypodium distachyon* roots. (A) Root tissue was sampled just prior to touch (t = 0), and at 10, 30, and 60 min following touch treatment in wildtype and *SWIZ-OE.* (B) Principal component analysis of gene expression across samples shows the greatest difference corresponding to genotype and the second greatest corresponding to time after touch. (C) Canonical, as well as novel touch responsive genes are upregulated in *B. distachyon* following touch. Closest orthologs of the *Arabidopsis thaliana TOUCH* genes encoding calmodulin-like (CML) and xyloglucan endo-transglycosylase/hydrolases (XTH) are upregulated following touch, as are previously unreported members of the glycosyl hydrolase 17 (GH17) family. Full list of gene expression for *TOUCH* and glycoside hydrolases defined by Tyler et al. (2010) in Supplemental Tables 5, 6,and 7. Significance denoted by * reflecting q < 0.1 compared to expression at t = 0, with q-values representing Wald test p-values adjusted for false discovery rate.

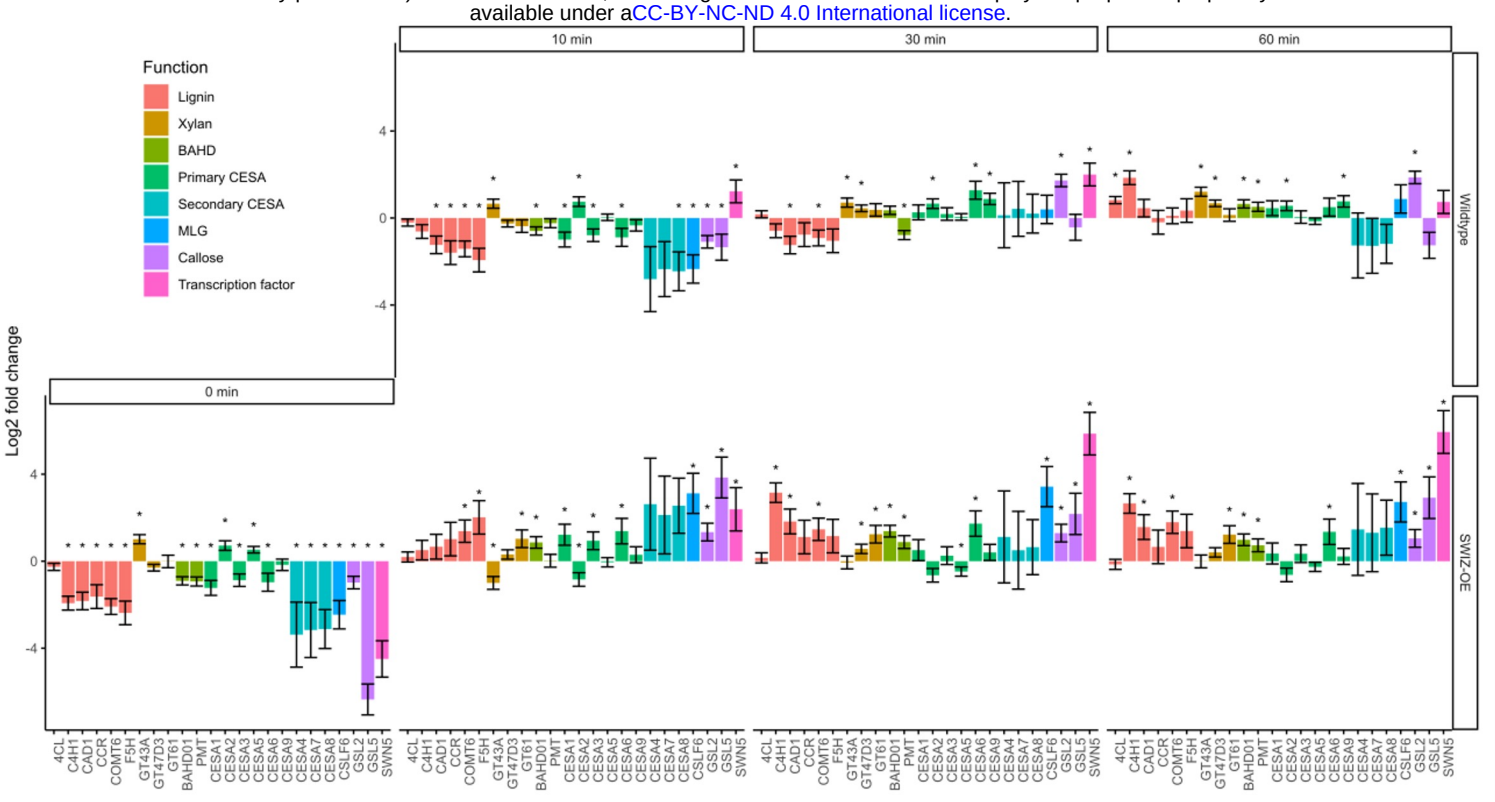

Figure 4. Gene expression analysis of cell wall related genes. Log fold-change of gene expression measured by RNA-seq in wildtype and *SWIZ-OE*, presented as relative to wildtype expression at time 0, pre-touch. Bar color indicates class of cell wall gene. Error bars indicate standard deviation of three biological replicates. Significance denoted by * reflecting $q < 0.1$ compared to wildtype expression at $t = 0$, with q-values representing Wald test p-values adjusted for false discovery rate. Legend abbreviations: BAHD, BAHD (BEAT, AHCT, HCBT, and DAT) acyltransferases; CESA, cellulose synthase; MLG, mixed-linkage glucans.

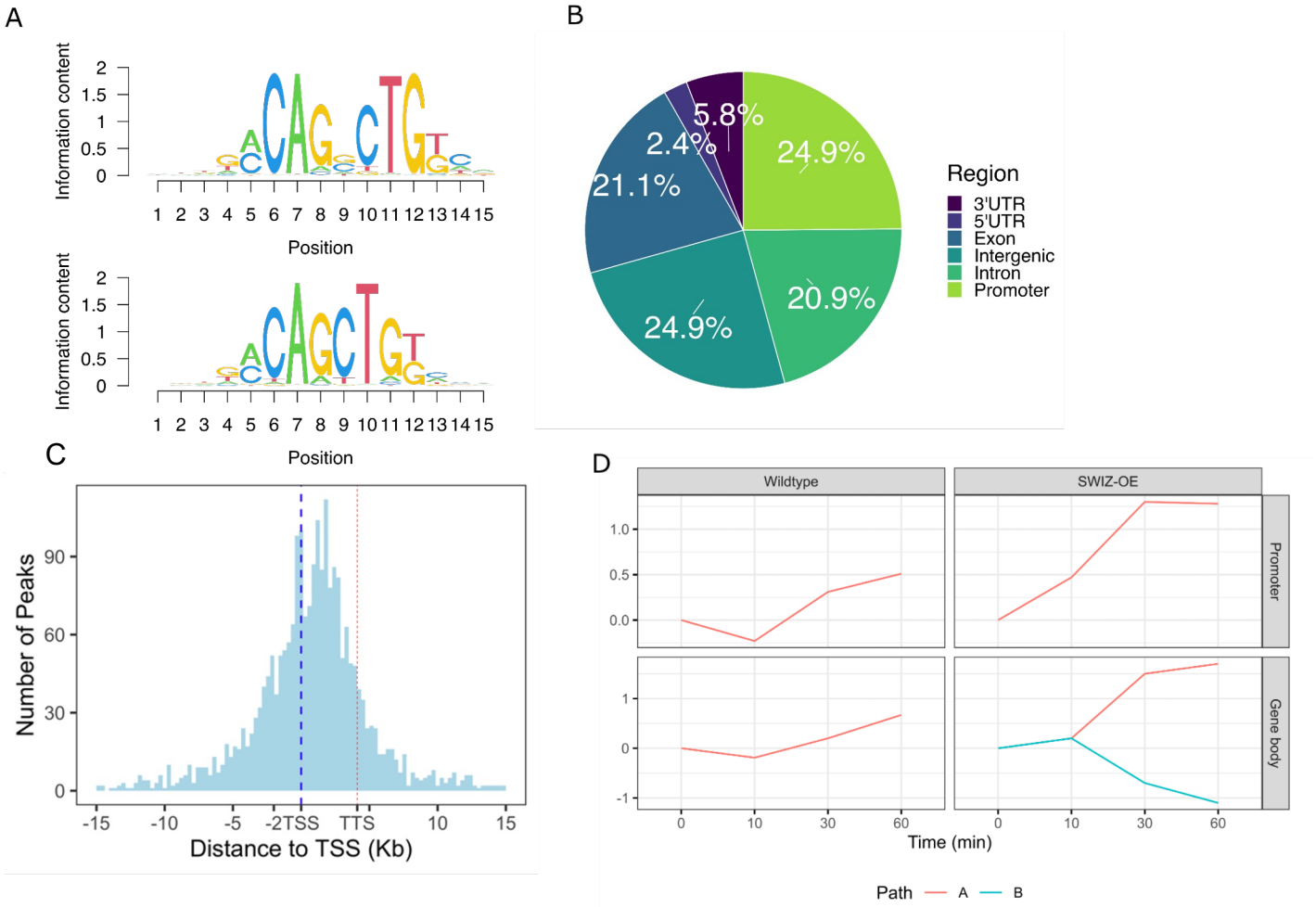

Figure 5. DNA affinity purification sequencing to determine SWIZ binding sites. (A) Top two most statistically enriched sequence motifs in SWIZ binding sites. (B) Distribution of binding sites across genomic features, relative to primary transcripts of the *Brachypodium distachyon* annotation v 3.1. (C) Relative distribution of binding sites centered on the transcriptional start site (TSS, blue dashed line), transcriptional termination site (TTS, red dashed line) represents the average length of all annotated transcripts, approximately 4.5 kb away from the TSS. (D) Path determinations from iDREM time course analysis of differentially expressed genes that also have DAP-seq binding sites. Each line represents a set of genes with similar expression level patterns over the time course relative to time 0, pre-touch.

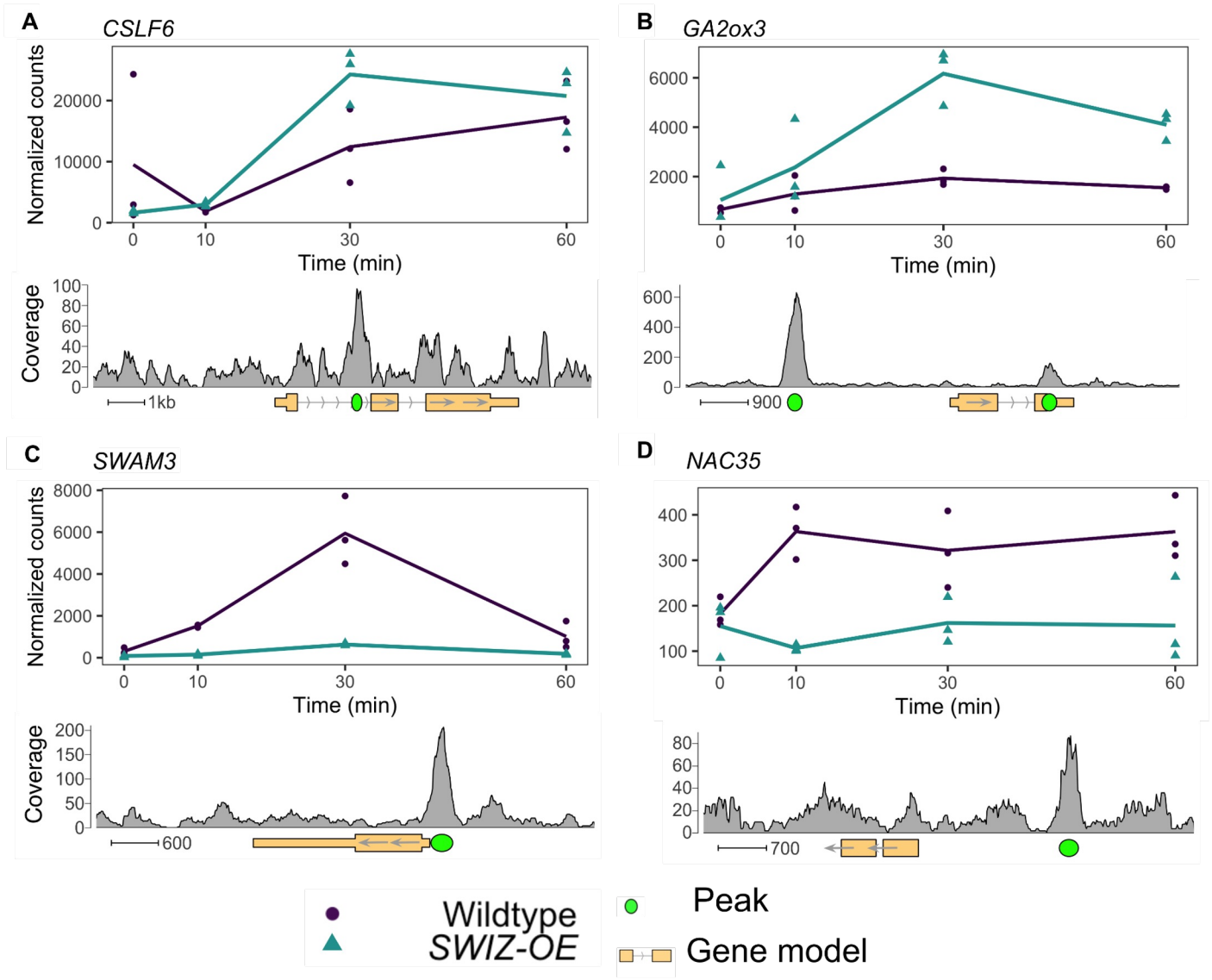

Figure 6. SWIZ binding targets differentially expressed in response to touch and *SWIZ-OE*. Gene expression over time of selected genes with SWIZ binding sites. Line graphs are the average transcript abundance of three biological replicates for each time point. Binding site determined as peaks of sequence alignment. Scale bar unit is bases. Direction of transcription is shown with arrows on the gene model, 5' and 3' UTRs are depicted by narrowed rectangles on the gene model.

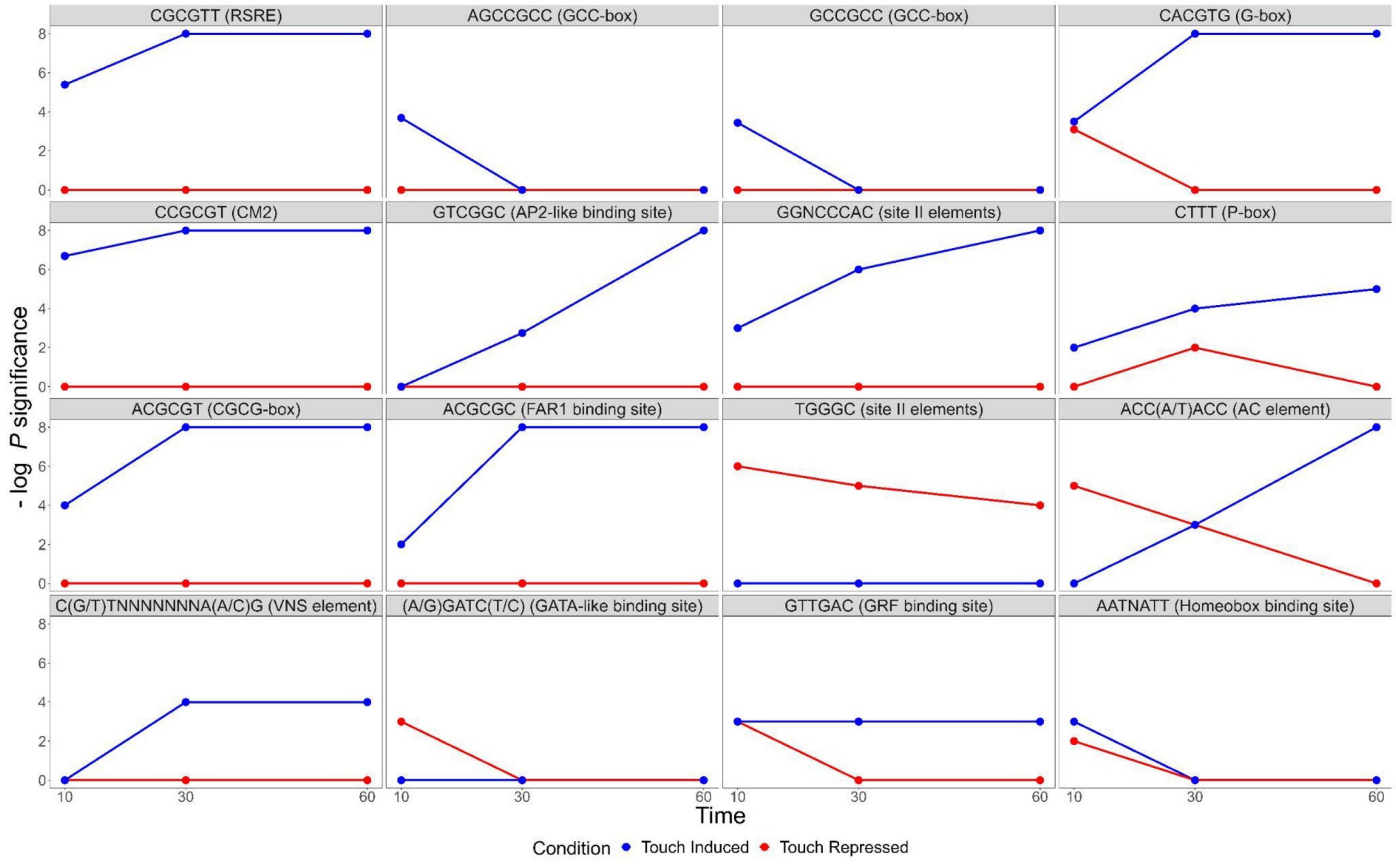

Figure 7. Sequence motifs enriched in the *cis*-regulatory regions of touch responsive *Brachypodium distachyon* genes. Negative log *p*-values for *cis*-elements, known and not known to be touch responsive. RSRE - Rapid Stress Response Element, FAR1 - FAR-RED impaired response1, GRF - Growth Regulating Factor, VNS - VND, NST/SND, SMB.

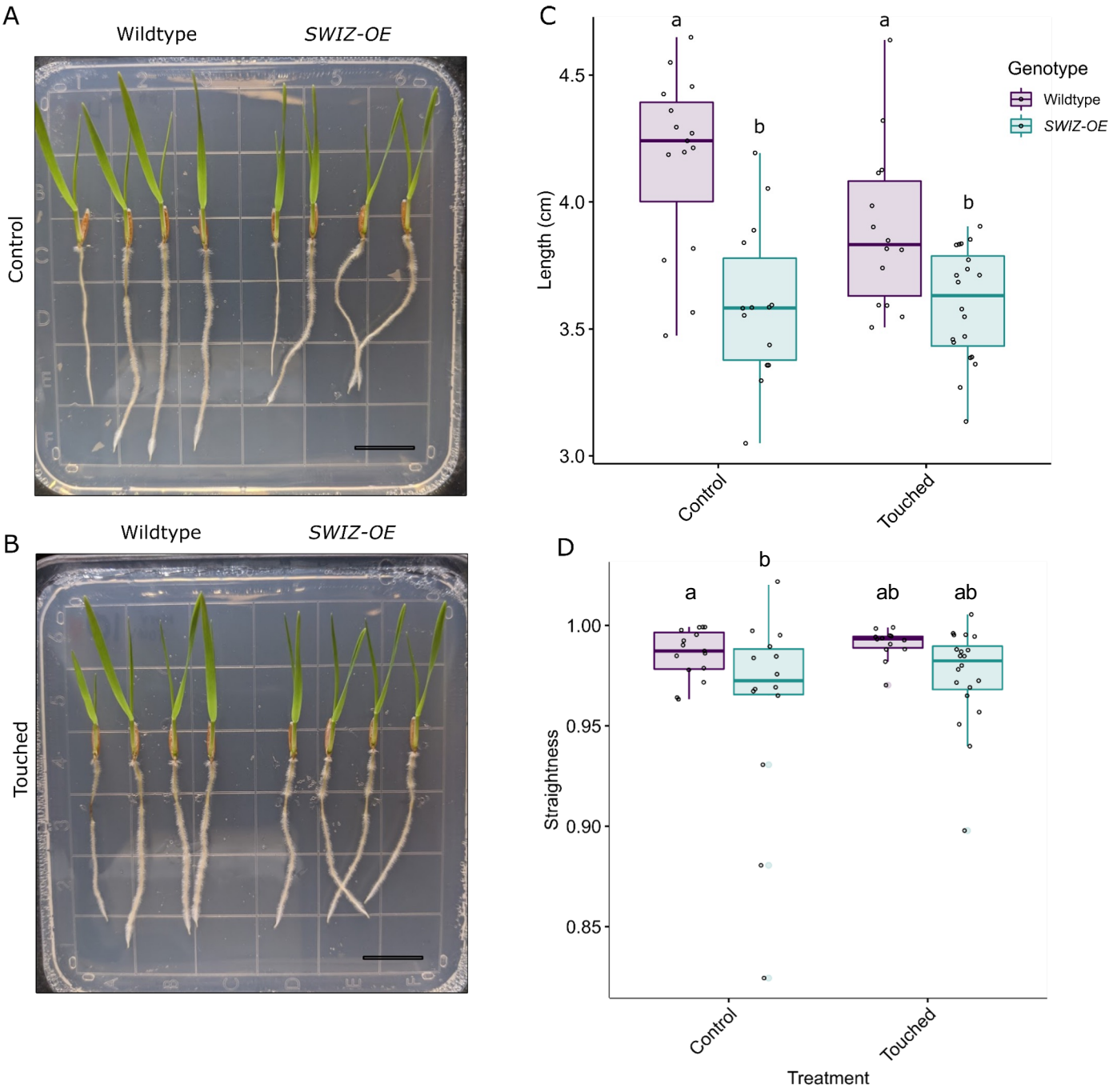

Figure 8. *SWIZ-OE* roots are shorter than wildtype with no significant difference in straightness in response to direct touch. Wildtype and *SWIZ-OE* seedlings grown on plates under control (A) or touched (B) conditions for five days. Touched plants were probed with a pipette tip twice a day. (C) Quantification of root length in control and touched conditions. Significance denoted by compact letter display reflecting Tukey HSD adjusted *p* values < 0.05. (D) Quantification of root straightness in control and touch conditions. Significance denoted by * reflecting Wilcoxon sign-ranked test for non-parametric data with *p*-value < 0.05, ns = not significant. Scale bar = 1 cm.

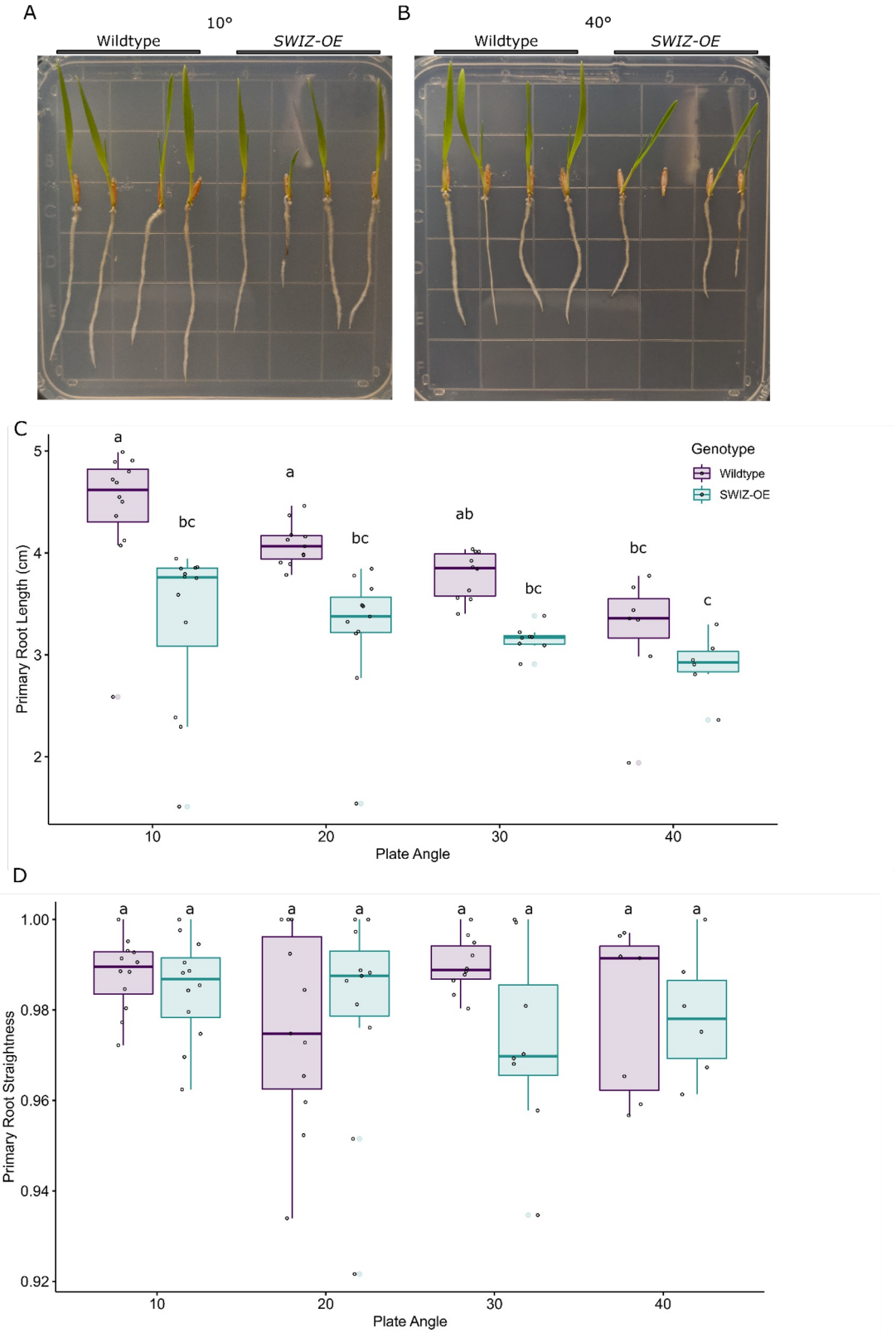

Figure 9. Wildtype roots shorten with increasing plate angle, while *SWIZ-OE* roots are consistently short, with no significant difference in straightness. Wildtype and *SWIZ-OE* seedlings grown on plates at (A) 10°, 20°, 30°, and (B) 40° incline from vertical. (C) Quantification of root length. (D) Quantification of primary root straightness. Significance denoted by compact letter display reflecting Tukey HSD adjusted *p*-values < 0.05. Scale bar = 1 cm.

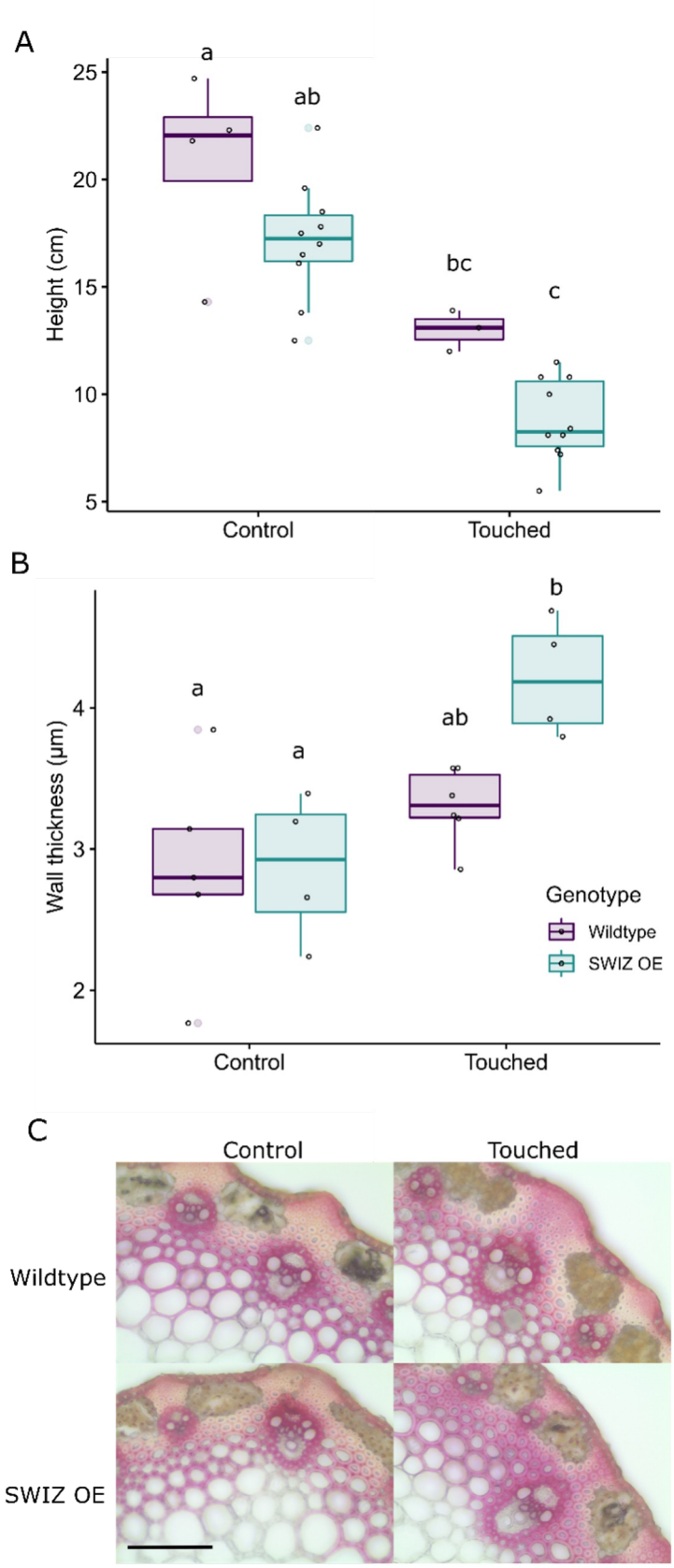

Figure 10. *SWIZ-OE* marginally enhanced thigmomorphogenic response in stems. Wildtype and *SWIZ-OE* plants were placed under control conditions or received two weeks of mechanical stress every 90 min. (A) Quantification of main stem height at senescence. (B) Quantification of interfascicular fiber wall thickness in transverse cross sections of the peduncle. n = 4 to 6 plants per genotype, per treatment. (C) Representative cross sections stained with phloroglucinol-HCl. Scale bar = 100 µm. Significance denoted by compact letter display reflecting Tukey HSD adjusted *p*-values < 0.05.

Parsed Citations

Altartouri B, Bidhendi AJ, Tani T, Suzuki J, Conrad C, Chebli Y, Liu N, Karunakaran C, Scarcelli G, Geitmann A (2019) Pectin chemistry and cellulose crystallinity govern pavement cell morphogenesis in a multi-step mechanism. Plant Physiol 181: 127–141
Google Scholar: Author Only Title Only Author and Title

Andrews S (2010) FastQC: a quality control tool for high throughput sequence data. http://www.bioinformatics.babraham.ac.uk/projects/fastqc:
Google Scholar: Author Only Title Only Author and Title

Bidhendi AJ, Altartouri B, Gosselin FP, Geitmann A (2019) Mechanical stress initiates and sustains the morphogenesis of wavy leaf epidermal cells. Cell Rep 28: 1237–1250.e6
Google Scholar: Author Only Title Only Author and Title

Bidhendi AJ, Geitmann A (2018) Finite element modeling of shape changes in plant cells. Plant Physiol 176: 41–56
Google Scholar: Author Only Title Only Author and Title

Biro RL, Hunt ER, Erner Y, Jaffe MJ (1980) Thigmomorphogenesis: changes in cell division and elongation in the internodes of mechanically-perturbed or ethrel-treated bean plants. Ann Bot 45: 655–664
Google Scholar: Author Only Title Only Author and Title

Börnke F, Rocksch T (2018) Thigmomorphogenesis – Control of plant growth by mechanical stimulation. Sci Hortic 234: 344–353
Google Scholar: Author Only Title Only Author and Title

Braam J (2004) In touch: plant responses to mechanical stimuli. New Phytol 165: 373–389
Google Scholar: Author Only Title Only Author and Title

Braam J, Davis RW (1990) Rain-, wind-, and touch-induced expression of calmodulin and calmodulin-related genes in Arabidopsis. Cell 60: 357–364
Google Scholar: Author Only Title Only Author and Title

Chehab EW, Eich E, Braam J (2009) Thigmomorphogenesis: a complex plant response to mechano-stimulation. J Exp Bot 60: 43–56
Google Scholar: Author Only Title Only Author and Title

Coomey JH, Sibout R, Hazen SP (2020) Grass secondary cell walls, Brachypodium distachyon as a model for discovery. New Phytol 227: 1709–1724
Google Scholar: Author Only Title Only Author and Title

Coutand C, Martin L, Leblanc-Fournier N, Decourteix M, Julien J-L, Moulia B (2009) Strain mechanosensing quantitatively controls diameter growth and PtaZFP2 gene expression in poplar. Plant Physiol 151: 223–232
Google Scholar: Author Only Title Only Author and Title

Deppmann CD, Acharya A, Rishi V, Wobbes B, Smeekens S, Taparowsky EJ, Vinson C (2004) Dimerization specificity of all 67 B-ZIP motifs in Arabidopsis thaliana: a comparison to Homo sapiens B-ZIP motifs. Nucleic Acids Res 32: 3435–3445
Google Scholar: Author Only Title Only Author and Title

Ding J, Hagood JS, Ambalavanan N, Kaminski N, Bar-Joseph Z (2018) iDREM: Interactive visualization of dynamic regulatory networks. PLoS Comput Biol 14: e1006019
Google Scholar: Author Only Title Only Author and Title

Doherty CJ, Van Buskirk HA, Myers SJ, Thomashow MF (2009) Roles for Arabidopsis CAMTA transcription factors in cold-regulated gene expression and freezing tolerance. Plant Cell 21: 972–984
Google Scholar: Author Only Title Only Author and Title

Dröge-Laser W, Snoek BL, Snel B, Weiste C (2018) The Arabidopsis bZIP transcription factor family-an update. Curr Opin Plant Biol 45: 36–49
Google Scholar: Author Only Title Only Author and Title

Ehlert A, Weltmeier F, Wang X, Mayer CS, Smeekens S, Vicente-Carbajosa J, Dröge-Laser W (2006) Two-hybrid protein-protein interaction analysis in Arabidopsis protoplasts: establishment of a heterodimerization map of group C and group S bZIP transcription factors. Plant J 46: 890–900
Google Scholar: Author Only Title Only Author and Title

Fernández-Calvo P, Chini A, Fernández-Barbero G, Chico J-M, Gimenez-Ibanez S, Geerinck J, Eeckhout D, Schweizer F, Godoy M, Franco-Zorrilla JM, et al (2011) The Arabidopsis bHLH transcription factors MYC3 and MYC4 are targets of JAZ repressors and act additively with MYC2 in the activation of jasmonate responses. Plant Cell 23: 701–715
Google Scholar: Author Only Title Only Author and Title

Fukazawa J, Nakata M, Ito T, Matsushita A, Yamaguchi S, Takahashi Y (2011) bZIP transcription factor RSG controls the feedback

regulation of NtGA20ox1 via intracellular localization and epigenetic mechanism. Plant Signal Behav 6: 26–28
Google Scholar: Author Only Title Only Author and Title

Fukazawa J, Nakata M, Ito T, Yamaguchi S, Takahashi Y (2010) The transcription factor RSG regulates negative feedback of NtGA20ox1 encoding GA 20-oxidase. Plant J 62: 1035–1045
Google Scholar: Author Only Title Only Author and Title

Fukazawa J, Sakai T, Ishida S, Yamaguchi I, Kamiya Y, Takahashi Y (2000) Repression of shoot growth, a bZIP transcriptional activator, regulates cell elongation by controlling the level of gibberellins. Plant Cell 12: 901–915
Google Scholar: Author Only Title Only Author and Title

Gibalová A, Steinbachová L, Hafidh S, Bláhová V, Gadiou Z, Michailidis C, Műller K, Pleskot R, Dupľáková N, Honys D (2017) Characterization of pollen-expressed bZIP protein interactions and the role of ATbZIP18 in the male gametophyte. Plant Reprod 30: 1–17
Google Scholar: Author Only Title Only Author and Title

Gladala-Kostarz A, Doonan JH, Bosch M (2020) Mechanical stimulation in Brachypodium distachyon: implications for fitness, productivity and cell wall properties. Plant Cell Environ 43: 1314–1330
Google Scholar: Author Only Title Only Author and Title

Grigoryan G, Keating AE (2006) Structure-based prediction of bZIP partnering specificity. J Mol Biol 355: 1125–1142
Google Scholar: Author Only Title Only Author and Title

Hamant O, Heisler MG, Jönsson H, Krupinski P, Uyttewaal M, Bokov P, Corson F, Sahlin P, Boudaoud A, Meyerowitz EM, et al (2008) Developmental patterning by mechanical signals in Arabidopsis. Science 322: 1650–1655
Google Scholar: Author Only Title Only Author and Title

Handakumbura P, Matos D, Osmont K, Harrington M, Heo K, Kafle K, Kim S, Baskin T, Hazen S (2013) Perturbation of Brachypodium distachyon CELLULOSE SYNTHASE A4 or 7 results in abnormal cell walls. BMC Plant Biol 13: 131
Google Scholar: Author Only Title Only Author and Title

Handakumbura PP, Brow K, Whitney IP, Zhao K, Sanguinet KA, Lee SJ, Olins J, Romero-Gamboa SP, Harrington MJ, Bascom CJ, et al (2018) SECONDARY WALL ASSOCIATED MYB1 is a positive regulator of secondary cell wall thickening in Brachypodium distachyon and is not found in the Brassicaceae. Plant J 96: 485–699
Google Scholar: Author Only Title Only Author and Title

Heinz S, Benner C, Spann N, Bertolino E, Lin YC, Laslo P, Cheng JX, Murre C, Singh H, Glass CK (2010) Simple combinations of lineage-determining transcription factors prime cis-regulatory elements required for macrophage and B cell identities. Mol Cell 38: 576–589
Google Scholar: Author Only Title Only Author and Title

Igarashi D, Ishida S, Fukazawa J, Takahashi Y (2001) 14-3-3 proteins regulate intracellular localization of the bZIP transcriptional activator RSG. Plant Cell 13: 2483–2497
Google Scholar: Author Only Title Only Author and Title

Iida H (2014) Mugifumi, a beneficial farm work of adding mechanical stress by treading to wheat and barley seedlings. Front Plant Sci 5: 453
Google Scholar: Author Only Title Only Author and Title

Ishida S, Fukazawa J, Yuasa T, Takahashi Y (2004) Involvement of 14-3-3 signaling protein binding in the functional regulation of the transcriptional activator REPRESSION OF SHOOT GROWTH by gibberellins. Plant Cell 16: 2641–2651
Google Scholar: Author Only Title Only Author and Title

Ishida S, Yuasa T, Nakata M, Takahashi Y (2008) A tobacco calcium-dependent protein kinase, CDPK1, regulates the transcription factor REPRESSION OF SHOOT GROWTH in response to gibberellins. Plant Cell 20: 3273–3288
Google Scholar: Author Only Title Only Author and Title

Ito T, Ishida S, Oe S, Fukazawa J, Takahashi Y (2017) Autophosphorylation affects substrate-binding affinity of tobacco Ca2+-dependent protein kinase1. Plant Physiol 174: 2457–2468
Google Scholar: Author Only Title Only Author and Title

Ito T, Nakata M, Fukazawa J, Ishida S, Takahashi Y (2014) Scaffold function of Ca2+-dependent protein kinase: tobacco Ca2+-DEPENDENT PROTEIN KINASE1 transfers 14-3-3 to the substrate REPRESSION OF SHOOT GROWTH after phosphorylation. Plant Physiol 165: 1737–1750
Google Scholar: Author Only Title Only Author and Title

Jaffe MJ (1973) Thigmomorphogenesis: The response of plant growth and development to mechanical stimulation : With special reference to Bryonia dioica. Planta 114: 143–157
Google Scholar: Author Only Title Only Author and Title

Jaffe MJ, Biro R, Bridle K (1980) Thigmomorphogenesis: Calibration of the parameters of the sensory function in beans. Physiol Plant 49: 410–416
Google Scholar: Author Only Title Only Author and Title

Jakoby M, Weisshaar B, Dröge-Laser W, Vicente-Carbajosa J, Tiedemann J, Kroj T, Parcy F, bZIP Research Group (2002) bZIP transcription factors in Arabidopsis. Trends Plant Sci 7: 106–111
Google Scholar: Author Only Title Only Author and Title

Katoh K, Rozewicki J, Yamada KD (2019) MAFFT online service: multiple sequence alignment, interactive sequence choice and visualization. Brief Bioinform 20: 1160–1166
Google Scholar: Author Only Title Only Author and Title

Kim D, Langmead B, Salzberg SL (2015) HISAT: a fast spliced aligner with low memory requirements. Nat Methods 12: 357
Google Scholar: Author Only Title Only Author and Title

Kim W-C, Ko J-H, Han K-H (2012) Identification of a cis-acting regulatory motif recognized by MYB46, a master transcriptional regulator of secondary wall biosynthesis. Plant Mol Biol 78: 489–501
Google Scholar: Author Only Title Only Author and Title

Leblanc-Fournier N, Martin L, Lenne C, Decourteix M (2014) To respond or not to respond, the recurring question in plant mechanosensitivity. Front Plant Sci 5: 401
Google Scholar: Author Only Title Only Author and Title

Lee D, Polisensky DH, Braam J (2005) Genome-wide identification of touch- and darkness-regulated Arabidopsis genes: a focus on calmodulin-like and XTH genes. New Phytol 165: 429–444
Google Scholar: Author Only Title Only Author and Title

Lee H-J, Kim H-S, Park JM, Cho HS, Jeon JH (2019) PIN-mediated polar auxin transport facilitates root obstacle avoidance. New Phytol. doi: 10.1111/nph.16076
Google Scholar: Author Only Title Only Author and Title

Lee TG, Jang CS, Kim JY, Kim DS, Park JH, Kim DY, Seo YW (2006) A Myb transcription factor (TaMyb1) from wheat roots is expressed during hypoxia: roles in response to the oxygen concentration in root environment and abiotic stresses. Physiol Plant 129: 375–385
Google Scholar: Author Only Title Only Author and Title

Li H, Handsaker B, Wysoker A, Fennell T, Ruan J, Homer N, Marth G, Abecasis G, Durbin R, 1000 Genome Project Data Processing Subgroup (2009) The Sequence Alignment/Map format and SAMtools. Bioinformatics 25: 2078–2079
Google Scholar: Author Only Title Only Author and Title

Liu R, Finlayson SA (2019) Sorghum tiller bud growth is repressed by contact with the overlying leaf. Plant Cell Environ 42: 2120–2132
Google Scholar: Author Only Title Only Author and Title

Liu X, Chu Z (2015) Genome-wide evolutionary characterization and analysis of bZIP transcription factors and their expression profiles in response to multiple abiotic stresses in Brachypodium distachyon. BMC Genomics 16: 227
Google Scholar: Author Only Title Only Author and Title

Lobet G, Pagès L, Draye X (2011) A novel image-analysis toolbox enabling quantitative analysis of root system architecture. Plant Physiol 157: 29–39
Google Scholar: Author Only Title Only Author and Title

Lourenço TF, Serra TS, Cordeiro AM, Swanson SJ, Gilroy S, Saibo NJM, Oliveira MM (2015) The Rice E3-Ubiquitin Ligase HIGH EXPRESSION OF OSMOTICALLY RESPONSIVE GENE1 Modulates the Expression of ROOT MEANDER CURLING, a Gene Involved in Root Mechanosensing, through the Interaction with Two ETHYLENE-RESPONSE FACTOR Transcription Factors. Plant Physiol 169: 2275–2287
Google Scholar: Author Only Title Only Author and Title

Love MI, Huber W, Anders S (2014) Moderated estimation of fold change and dispersion for RNA-seq data with DESeq2. Genome Biol 15: 550
Google Scholar: Author Only Title Only Author and Title

MacKinnon KJ-M, Cole BJ, Yu C, Coomey JH, Hartwick NT, Remigereau M-S, Duffy T, Michael TP, Kay SA, Hazen SP (2020) Changes in ambient temperature are the prevailing cue in determining Brachypodium distachyon diurnal gene regulation. New Phytol 227: 1649–1667
Google Scholar: Author Only Title Only Author and Title

Martin L, Leblanc-Fournier N, Julien J-L, Moulia B, Coutand C (2010) Acclimation kinetics of physiological and molecular responses of plants to multiple mechanical loadings. J Exp Bot 61: 2403–2412
Google Scholar: Author Only Title Only Author and Title

Matos DA, Whitney IP, Harrington MJ, Hazen SP (2013) Cell walls and the developmental anatomy of the Brachypodium distachyon stem internode. PLoS One 8: e80640
Google Scholar: Author Only Title Only Author and Title

McCahill IW, Hazen SP (2019) Regulation of cell wall thickening by a medley of mechanisms. Trends Plant Sci 24: 853–866
Google Scholar: Author Only Title Only Author and Title

Monshausen GB, Bibikova TN, Weisenseel MH, Gilroy S (2009) Ca2+ regulates reactive oxygen species production and pH during mechanosensing in Arabidopsis roots. Plant Cell 21: 2341–2356
Google Scholar: Author Only Title Only Author and Title

Moore BM, Lee YS, Wang P, Azodi C, Grotewold E, Shiu S-H (2022) Modeling temporal and hormonal regulation of plant transcriptional response to wounding. Plant Cell 34: 867–888
Google Scholar: Author Only Title Only Author and Title

Moulia B, Coutand C, Julien J-L (2015) Mechanosensitive control of plant growth: bearing the load, sensing, transducing, and responding. Front Plant Sci 6: 52
Google Scholar: Author Only Title Only Author and Title

Nam BE, Park Y-J, Gil K-E, Kim J-H, Kim JG, Park C-M (2020) Auxin mediates the touch-induced mechanical stimulation of adventitious root formation under windy conditions in Brachypodium distachyon. BMC Plant Biol 20: 335
Google Scholar: Author Only Title Only Author and Title

Niez B, Dlouha J, Moulia B, Badel E (2019) Water-stressed or not, the mechanical acclimation is a priority requirement for trees. Trees 33: 279–291
Google Scholar: Author Only Title Only Author and Title

Ohtani M, Nishikubo N, Xu B, Yamaguchi M, Mitsuda N, Goué N, Shi F, Ohme-Takagi M, Demura T (2011) A NAC domain protein family contributing to the regulation of wood formation in poplar. Plant J 67: 499–512
Google Scholar: Author Only Title Only Author and Title

Olins JR, Lin L, Lee SJ, Trabucco GM, MacKinnon KJM, Hazen SP (2018) Secondary wall regulating NACs differentially bind at the promoter at a CELLULOSE SYNTHASE A4 cis-eQTL. Front Plant Sci 9: 1895
Google Scholar: Author Only Title Only Author and Title

Oliva M, Dunand C (2007) Waving and skewing: how gravity and the surface of growth media affect root development in Arabidopsis. New Phytol 176: 37–43
Google Scholar: Author Only Title Only Author and Title

O'Malley RC, Huang S-SC, Song L, Lewsey MG, Bartlett A, Nery JR, Galli M, Gallavotti A, Ecker JR (2016) Cistrome and epicistrome features shape the regulatory DNA landscape. Cell 165: 1280–1292
Google Scholar: Author Only Title Only Author and Title

Pertea M, Pertea GM, Antonescu CM, Chang T-C, Mendell JT, Salzberg SL (2015) StringTie enables improved reconstruction of a transcriptome from RNA-seq reads. Nat Biotechnol 33: 290–295
Google Scholar: Author Only Title Only Author and Title

Pitzschke A, Djamei A, Teige M, Hirt H (2009) VIP1 response elements mediate mitogen-activated protein kinase 3-induced stress gene expression. Proc Natl Acad Sci U S A 106: 18414–18419
Google Scholar: Author Only Title Only Author and Title

Polisensky DH, Braam J (1996) Cold-shock regulation of the Arabidopsis TCH genes and the effects of modulating intracellular calcium levels. Plant Physiol 111: 1271–1279
Google Scholar: Author Only Title Only Author and Title

Pomiès L, Decourteix M, Franchel J, Moulia B, Leblanc-Fournier N (2017) Poplar stem transcriptome is massively remodelled in response to single or repeated mechanical stimuli. BMC Genomics 18: 300
Google Scholar: Author Only Title Only Author and Title

Raudvere U, Kolberg L, Kuzmin I, Arak T, Adler P, Peterson H, Vilo J (2019) g:Profiler: a web server for functional enrichment analysis and conversions of gene lists. Nucleic Acids Res 47: W191–W198
Google Scholar: Author Only Title Only Author and Title

Ringli C, Keller B (1998) Specific interaction of the tomato bZIP transcription factor VSF-1 with a non-palindromic DNA sequence that controls vascular gene expression. Plant Mol Biol 37: 977–988
Google Scholar: Author Only Title Only Author and Title

Roignant J, Badel É, Leblanc-Fournier N, Brunel-Michac N, Ruelle J, Moulia B, Decourteix M (2018) Feeling stretched or compressed? The multiple mechanosensitive responses of wood formation to bending. Ann Bot 121: 1151–1161
Google Scholar: Author Only Title Only Author and Title

Rushton PJ, Reinstädler A, Lipka V, Lippok B, Somssich IE (2002) Synthetic plant promoters containing defined regulatory elements provide novel insights into pathogen- and wound-induced signaling. Plant Cell 14: 749–762
Google Scholar: Author Only Title Only Author and Title

Schütze K, Harter K, Chaban C (2008) Post-translational regulation of plant bZIP factors. Trends Plant Sci 13: 247–255
Google Scholar: Author Only Title Only Author and Title

Shah L, Yahya M, Shah SMA, Nadeem M, Ali A, Ali A, Wang J, Riaz MW, Rehman S, Wu W, et al (2019) Improving lodging resistance: using wheat and rice as classical examples. Int J Mol Sci. doi: 10.3390/ijms20174211
Google Scholar: Author Only Title Only Author and Title

Sibout R, Proost S, Hansen BO, Vaid N, Giorgi FM, Ho-Yue-Kuang S, Legée F, Cézart L, Bouchabké-Coussa O, Soulhat C, et al (2017) Expression atlas and comparative coexpression network analyses reveal important genes involved in the formation of lignified cell wall in Brachypodium distachyon. New Phytol 215: 1009–1025
Google Scholar: Author Only Title Only Author and Title

Swanson SJ, Barker R, Ye Y, Gilroy S (2015) Evaluating mechano-transduction and touch responses in plant roots. Methods Mol Biol 1309: 143–150
Google Scholar: Author Only Title Only Author and Title

Szczegielniak J, Borkiewicz L, Szurmak B, Lewandowska-Gnatowska E, Statkiewicz M, Klimecka M, Cieśla J, Muszyńska G (2012) Maize calcium-dependent protein kinase (ZmCPK11): local and systemic response to wounding, regulation by touch and components of jasmonate signaling. Physiol Plant 146: 1–14
Google Scholar: Author Only Title Only Author and Title

Trabucco GM, Matos DA, Lee SJ, Saathoff A, Priest H, Mockler TC, Sarath G, Hazen SP (2013) Functional characterization of cinnamyl alcohol dehydrogenase and caffeic acid O-methyltransferase in Brachypodium distachyon. BMC Biotechnol 13: 61
Google Scholar: Author Only Title Only Author and Title

Trifinopoulos J, Nguyen L-T, von Haeseler A, Minh BQ (2016) W-IQ-TREE: a fast online phylogenetic tool for maximum likelihood analysis. Nucleic Acids Res 44: W232–W235
Google Scholar: Author Only Title Only Author and Title

Tsugama D, Liu S, Fujino K, Takano T (2018) Calcium signalling regulates the functions of the bZIP protein VIP1 in touch responses in Arabidopsis thaliana. Ann Bot 122: 1219–1229
Google Scholar: Author Only Title Only Author and Title

Tsugama D, Liu S, Takano T (2012) A bZIP protein, VIP1, is a regulator of osmosensory signaling in Arabidopsis. Plant Physiol 159: 144–155
Google Scholar: Author Only Title Only Author and Title

Tsugama D, Liu S, Takano T (2016) The bZIP protein VIP1 Is involved in touch responses in Arabidopsis roots. Plant Physiol 171: 1355–1365
Google Scholar: Author Only Title Only Author and Title

Tsugama D, Liu S, Takano T (2014) Analysis of functions of VIP1 and its close homologs in osmosensory responses of Arabidopsis thaliana. PLoS One 9: e103930
Google Scholar: Author Only Title Only Author and Title

Tyler L, Bragg JN, Wu J, Yang X, Tuskan GA, Vogel JP (2010) Annotation and comparative analysis of the glycoside hydrolase genes in Brachypodium distachyon. BMC Genomics 11: 600
Google Scholar: Author Only Title Only Author and Title

Uyttewaal M, Burian A, Alim K, Landrein B, Borowska-Wykręt D, Dedieu A, Peaucelle A, Ludynia M, Traas J, Boudaoud A, et al (2012) Mechanical stress acts via katanin to amplify differences in growth rate between adjacent cells in Arabidopsis. Cell 149: 439–451
Google Scholar: Author Only Title Only Author and Title

Valdivia ER, Herrera MT, Gianzo C, Fidalgo J, Revilla G, Zarra I, Sampedro J (2013) Regulation of secondary wall synthesis and cell death by NAC transcription factors in the monocot Brachypodium distachyon. J Exp Bot 64: 1333–1343
Google Scholar: Author Only Title Only Author and Title

Van Leene J, Blomme J, Kulkarni SR, Cannoot B, De Winne N, Eeckhout D, Persiau G, Van De Slijke E, Vercruysse L, Vanden Bossche R, et al (2016) Functional characterization of the Arabidopsis transcription factor bZIP29 reveals its role in leaf and root development. J Exp Bot 67: 5825–5840
Google Scholar: Author Only Title Only Author and Title

Van Moerkercke A, Duncan O, Zander M, Šimura J, Broda M, Vanden Bossche R, Lewsey MG, Lama S, Singh KB, Ljung K, et al (2019) A MYC2/MYC3/MYC4-dependent transcription factor network regulates water spray-responsive gene expression and jasmonate levels. Proc Natl Acad Sci U S A 116: 23345–23356

Google Scholar: Author Only Title Only Author and Title

Walley J, Coughlan S, Hudson ME, Covington MF, Kaspi R, Banu G, Harmer SL, Dehesh K (2007) Mechanical stress induces biotic and abiotic stress responses via a novel cis-element. PLoS Genet 3: 1800–1812

Google Scholar: Author Only Title Only Author and Title

Weltmeier F, Ehlert A, Mayer CS, Dietrich K, Wang X, Schütze K, Alonso R, Harter K, Vicente-Carbajosa J, Dröge-Laser W (2006) Combinatorial control of Arabidopsis proline dehydrogenase transcription by specific heterodimerisation of bZIP transcription factors. EMBO J 25: 3133–3143

Google Scholar: Author Only Title Only Author and Title

Yin Y, Zhu Q, Dai S, Lamb C, Beachy RN (1997) RF2a, a bZIP transcriptional activator of the phloem-specific rice tungro bacilliform virus promoter, functions in vascular development. EMBO J 16: 5247–5259

Google Scholar: Author Only Title Only Author and Title

Zha G, Wang B, Liu J, Yan J, Zhu L, Yang X (2016) Mechanical touch responses of Arabidopsis TCH1-3 mutant roots on inclined hard-agar surface. International Agrophysics 30: 65

Google Scholar: Author Only Title Only Author and Title

Zhong R, Lee C, McCarthy RL, Reeves CK, Jones EG, Ye Z-H (2011) Transcriptional activation of secondary wall biosynthesis by rice and maize NAC and MYB transcription factors. Plant Cell Physiol 52: 1856–1871

Google Scholar: Author Only Title Only Author and Title

Zhong R, Ye Z-H (2012) MYB46 and MYB83 bind to the SMRE sites and directly activate a suite of transcription factors and secondary wall biosynthetic genes. Plant Cell Physiol 53: 368–380

Google Scholar: Author Only Title Only Author and Title